SYNTHESIS AND CHARACTARIZATION OF CaO/AC FROM EGGSHELL AND BANANA PEELS WASTES FOR PHOTO-CATALYTIC APPLICATION

GELANE ABEBE FUFA

A THESIS SUBMITTED TO DEPARTMENT OF APPLIED CHEMISTRY SCHOOL OF APPLIED NATURAL SCIENCE

IN PARTIAL FULFILLMENT OF THE REQUIREMENTS FOR THE DEGREE OF MASTER OF SCIENCE IN APPLIED CHEMISTRY (ANALYTICAL CHEMISTRY)

OFFICE OF POST GRADUATE STUDIES
ADAMA SCIENCE AND TECHNOLOGY UNIVERSITY (ASTU)

JUNE, 2024
ADAMA, ETHIOPI

Synthesis and Characterization of CaO/AC from Eggshell and Banana Peels Wastes for Photo-catalytic Application

Gelane Abebe

Advisor: Gemechu Deressa (PhD, Associate Professor)

Co-Advisor: Defaru Negera (PhD, Assistant Professor)

A Thesis Proposal Submitted to Department of Applied Chemistry

School of Applied Natural Science

In Partial Fulfillment of the Requirements for the Degree of Master of Science in Applied Chemistry (Analytical Chemistry)

Office of Post Graduate Studies

Adama Science and Technology University (ASTU)

JUNE, 2024

Adama, Ethiopia

DECLARATION

I declare that this thesis titled "**Synthesis and Characterization of CaO/AC from Eggshell and Banana Peels Wastes for Photo-catalytic Application**" is my work and has not been submitted to any university for similar purposes. The references used in this Thesis are duly recognized by proper citation.

Gelane Abebe	_____	_____
Name of student	Signature	Date

RECOMMENDATION

We, the major and co-advisors of this thesis, hereby certify that we have closely advised the student while developing this Thesis and have read the draft of the thesis entitled with "**Synthesis and Characterization of CaO/AC from Eggshell and Banana Peels Wastes for Photo-catalytic Application**" prepared under my guidance by **Gelane Abebe**. Therefore, we recommend the submission of the research Thesis to the department for further review and evaluation.

Dr Gemechu Deressa	_____	_____
Major Advisor	Signature	Date
Dr. Defaru Negera	_____	_____
Co-advisor	Signature	Date

APPROVAL

The advisors hereby certify that the recommendation and suggestions given by the Thesis review committee are appropriately incorporated into the final thesis entitled "**Synthesis and Characterization of CaO/AC from Eggshell and Banana Peels Wastes for Photo-catalytic Application**" by **Gelane Abebe**.

Dr Gemechu Deressa	_____	_____
Major Advisor	Signature	Date
Dr. Defaru Negera	_____	_____
Co-advisor	Signature	Date

APPROVAL OF BOARD OF REVIEWERS

We, the undersigned, members of the Board of Examiners of the thesis by **GELANE ABEBE** have read and evaluated the thesis entitled "**Synthesis and Characterization of CaO/AC from Eggshell and Banana Peels Wastes for Photo-catalytic Application**" and examined the candidate during open defense. This is, therefore, to certify that the thesis is accepted for partial fulfillment of the requirement of the degree of Master of Science in Applied Chemistry **(Analytical Chemistry).**

Dr. Worku Dinku	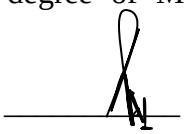	June 28, 2024
Chairperson	Signature	Date
Dr. Mengistu Woldetinsay	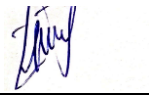	June 28,2024
Reviewer 1	Signature	Date
Dr.Hizkeal Tsade	_____	_____
Reviewer 2	Signature	Date

Final approval and acceptance of the thesis is contingent upon submission of its final copy to the Office of Postgraduate Studies (OPGS) through the Department Graduate Council (DGC) and School Graduate Committee (SGC).

_____	_____	_____
Department Head	Signature	Date
_____	_____	_____
School Dean	Signature	Date
_____	_____	_____
Office of Postgraduate Studies, Dean	Signature	Date

ACKNOWLEDGEMENT

First, I would like to thank God the almighty, for letting me through all the difficulties. I have experienced his guidance day by day. You are the one who let me finish my work. I would like to express my sincere gratitude to my advisor Dr. Gemechu Deressa who made this work possible by bringing his considerable experience and knowledge to this project. His guidance and advise carried me through all the stages of doing my work and writing my thesis, I am extremely grateful for your assistance and suggestion throughout my project. I am very grateful for my co-advisor Dr. Defaru Negera. I am sincerely express my gratitude to Dr. Hoden Ali Farah for letting me study the master's program in ASTU by recompense my full tuition feel and funding financial support and research fund to accomplish this research and I want to reiterate my deepest appreciation and also extend my thanks to Ms. Fikir Addise for her direct and indirect contributions that have significantly contributed to my successful achievements.

I also acknowledge Adama Science and Technology University (ASTU) for giving me the chance of MSc opportunity.

I thank Mr. Leta Guta laboratory technical in Applied Biology Department for helping me in scanning electron microscopy. I would like to thank Department of Applied Chemistry and laboratory technical Mr. Guta Amanu, and Mr. Girma Hailu, Material and Engineering Department and laboratory technical Mr. Demeke Tessfaye, Also, I want to thank Addis Ababa Science and Technology University for facilitating FTIR spectral analysis.

Finally, I would like to give my warmest thanks to my family and friends for their continuous support and understanding when undertaking my project, your prayer helps me survive all the stress from this year and not letting me give up.

TABLE OF CONTENTS

CONTENTS Page

LIST OF TABLES

LIST OF FIGURES

LIST OF ACRONYMS

AOP	Advanced oxidation processes
AC	Activated Carbon
EBT	Black-T
ES	Eggshell
FTIR	Fourier Transform Infrared
MB	Methylene Blue
NCs	Nanocomposites
NPs	Nanoparticles
PES	Preparation of Eggshell
RESP	Raw eggshell powder
SEM	Scanning electron microscopy
ROS	Reactive oxygen species
UV-vis	Ultraviolet-visible
XRD	X-ray diffraction

ABSTRACT

In this we study about environmental pollution is a major threat to human health and ecosystems, particularly when it comes to water pollution from industrial waste that contains organic dyes and other dangerous chemicals. The unregulated discharge of these pollutants into water bodies puts aquatic life in jeopardy and contaminates the water unfit for human consumption. Photo-catalysis, a technology that employs light to activate catalysts and break down pollutants into harmless chemicals, is one promising approach to solving this problem. By using this creative method to clean up contaminated water, industrial pollution can be prevented from having a negative impact on the environment and public health. W*e investigated the use of Calcium Oxide composite with Activated carbon (CaO/AC) synthesized from Eggshell (ES) and Banana peels(BP)) for the removal of methylene blue (MB) from wastewater. Pristine biomass of BP as its corresponding biochar-based nano composites were synthesized by pyrolyzing at 400°C for 1.5 hr. The TGA-DTA was used for thermal analysis. The result showed 800°C as the point at which stable metal oxide is formed. XRD was used for crystalline size determination. FTIR was determine functional group of compound and SEM was showed morphological surface of samples. Activated carbon was synthesized (AC) and characterized XRD crystalline. The synthesized CaO NPs and composite of CaO with AC were examined for photocatalytic dye degradation of dyes such as Methylene blue (MB) in aqueous medium. Where composite form of CaO with AC form the $CaCO_3$ due to calcination process in the presence of corbondyoxide (CO_2). The studies include optimization of parameter which found to be 12pH, 10ppm dye concentration and 10mg of catalyst loading were effective operation condition. The composite demonstrated a remarkable 98.76% degrading efficiency within $2.13*10^{-4}$ minute Uv visible irradiation. These optimized settings, highlighting its potential for effective wastewater treatment applications.*

Key words: Banana peels**,** Eggshell, CaO, CaO/AC, methyl blue, photo-catalyst**.**

1. INTRODUCTION

1.1 Background of the Study

Now a day human activity that cause in the degradation or depreciation of the quality of the natural environment is regarded as pollution(Ukaogo *et al*., 2020). In recent years, environmental pollution has been identified as one of the greatest problems concerning our society(Nadew *et al*., 2023). Such pollution refers to the contamination of the natural environment by various pollutants, leading to adverse effects on living organisms and ecosystems. Contamination of water can have a number of effects. The UN estimates that over 1.5 million people worldwide die from illnesses related to drinking water each year, and that one in three people lack access to clean drinking water(Mujtaba *et al*., 2023). The vast development of the textile industries has contributed a significant impact to water pollution, which is mainly due to the highly coloured effluents containing organic and inorganic dyes that have been disposed to the water stream(Ukaogo *et al*., 2020). Dyes are commonly used to color products in heavy industries such as textiles, paper, and food processing. Over 700,000 tons of dyes are produced annually worldwide, and there are about 100,000 distinct kinds of dyes that are used in different industries(Kochito *et al*., 2024). Many chemical processes, such as dyeing, bleaching, and finishing, are used in the textile industry to produce textiles, and these processes need a lot of water. Because of this, the textile sector produces large volumes of wastewater, which frequently contains dangerous chemicals and dyes. The release of untreated or insufficiently treated wastewater into bodies of water is one of the main causes of water pollution from the textile industries. High concentrations of dyes, heavy metals, solvents, and other hazardous materials are frequently found in this wastewater (Mujtaba *et al.*, 2023). Methylene blue (MB) is an organic dye that is widely used to color paper, print cotton, and dye leather and plastics. Long-term exposure to MB can endanger marine life by causing tissue necrosis and cyanosis. Industrial effluents that have been partially or not treated are released into the environment, allowing it to enter(Kochito *et al*., 2024).

To remove organic dyes and pigments from wastewater, physical, chemical, and biological techniques are being applied. Variety of techniques such as including adsorption, coagulation, precipitation, reverse osmosis, photo-degradation, electrochemical oxidation, and ozonation are

eliminating dyes(A. V. Borhade & Kale, 2017). One popular and successful technique for tackling the problem of water pollution is the elimination of organic dyes through photocatalytic degradation. In order to break down organic colors into simpler, less toxic chemicals like carbon dioxide and water, this method makes use of the catalytic qualities of materials like titanium dioxide when exposed to ultraviolet radiation. This method has the added benefit of not producing any hazardous byproducts or adding more chemicals to the environment. Since organic dyes are widely used in the food processing and textile industries, it is adaptable enough to treat wastewater from a variety of industries. Photocatalytic degradation provides an environmentally responsible way to meet water quality regulations, which are becoming more stringent globally (Borhade *et al.*, 2012).

Researchers investigations indicated that advanced oxidation processes (AOPs) using heterogeneous photo catalysis are the best alternative to conventional approaches for resolving this problems (Remucal & Manley, 2016). Application of Nano materials in AOP process improves the efficiency of dye degradation than bulk material due higher surface area. Higher surface area of nanoparticles results in production of large number of reactive species and there by increases the degradation efficiency. Heterogeneous photo catalysis with semiconducting metal oxide nanoparticles is one of the AOPs. They can degrade dye molecules in the water into less toxic components by the generation of electron hole pairs in this process.

Metal-oxide nanoparticles, such as calcium oxide (CaO), titanium (IV) oxide (TiO_2), zinc (II) oxide (ZnO), iron (III) oxide (Fe_2O_3), copper (II) oxide (CuO), nickel (II) oxide (NiO), and tin (IV) oxide (SnO_2), are now being investigated for their usage as photo catalyst to remove dyes (Kanade *et al.*, 2007). A large number of these compounds have broad band gaps, which reduces their ability to both absorb visible light and generate the electron-hole pairs required for photocatalytic activity. The difference in energy between a semiconductor's lowest unoccupied energy level (conduction band) and its highest occupied energy level (valence band) is known as one's band gap. In order for the semiconductor material to efficiently promote electrons from the valence band to the conduction band by photo catalysis, photons with energy equivalent to or greater than its band gap must be absorbed. Scholars have investigated a number of approaches to deal with the problem caused by large band gaps(Veeranna *et al.*, 2014).

Calcium oxide (CaO) nanoparticles derived from eggshell is used as photo catalyst for effective dye degradation, which is reutilization of kitchen waste (eggshell) in a sustained manner and is a cheaper catalyst than previously reported materials(Sree *et al.*, 2020).

Activated carbon (AC) is a carbonaceous material, and its complex network of internal pore structures, and sufficient functional groups, are used as adsorbents industrial from water pollution removal. The agro-industrial waste used as an alternative to develop low-cost adsorbents because of its abundantly available, biodegradable, renewable material, and high lignocellulosic composition(Maia *et al.*, 2021).

This technique is very effective at removing dyes from their aqueous medium while also being environmentally friendly. This inexpensive adsorbent is a very effective adsorbent for the removal of dyes such as murexide, eriochrome black T, and rhodamine B(A. V. Borhade & Kale, 2017).

Thus, the use of nanocomposites is more useful than single nanoparticles for the photocatalytic degradation of dyes. During the formation of nanocomposites there may be the formation of hetero-junctions between nanoparticles which reduces the electron-hole pair recombination, band gap and crystalline size. In order to achieve the desired photocatalytic activity, the composite's CaO to carbon ratio is essential. To maximize the photocatalytic performance and achieve synergistic effects, it is crucial to optimize the composition by balancing the amount of carbon and CaO. Researchers are exploring ways to overcome the limitation of photocatalytic degradation such as the law usage of visible light, fast charge recombination and low migrate ability of the photo generated electrons and holes(Chakhtouna *et al.*, 2021).

The purpose of this work was to synthesize and characterize CaO/AC nanocomposites in order to explore and develop them. This required dissecting their optical characteristics using methods like Fourier transform infrared spectroscopy (FT-IR) to pinpoint functional groups, scanning electron microscopy (SEM) to study their morphology at the nanoscale, X-ray diffraction (XRD) to ascertain their crystal structure, and ultraviolet-visible (UV-Vis) spectroscopy to comprehend how they interact with light. Also to evaluate the CaO/AC composite's and nanoparticles' photocatalytic performance. Their capacity to break down methylene blue, a common organic dye pollution, under various light conditions UV light and visible light irradiation was examined in order to undertake this evaluation. These evaluations are important because they shed light on

the possible uses of CaO/AC nanocomposites in environmental remediation, particularly in the treatment of organic dye-contaminated water.

1.2 Statement of Problem

The survival of humans depends on having access to clean water. One of the most important steps in lowering pollutants and environmental issues is wastewater treatment. In addition, wastewater recycling and reuse are essential to provide the water required for domestic, industrial, and irrigation uses due to the world's population expansion and economic development. One of the most efficient and low-cost ways to achieve this goal is through photocatalytic degradation of organic dyes. In order to successfully remove dangerous organic contaminants from industrial wastewater and handle serious environmental issues related to water contamination, photo-catalysis is a potential method. It is impossible to overestimate the significance of clean water for human survival, which is why effective wastewater treatment methods are desperately needed. Because photocatalytic degradation may use light energy to activate semiconductor materials, it is a very attractive technique. Semiconductor materials produce electron-hole pairs in response to light, which strongly react with their surfaces to cause oxidation and reduction. Complex organic pollutants, such as colors like methylene blue, can be broken down by this process into non-toxic substances like water and carbon dioxide. The use of extra chemicals is not required for photocatalysis to function, which reduces the risk of secondary contamination that comes with using traditional treatment techniques(Kuriakose *et al*., 2015). Methylene blue can be degraded more effectively through photo catalysis, although some of the photo catalysts used have a number of drawbacks, such as recombination of the photo generated electrons and electron holes, which slows down the rate of degradation (Saggioro *et al*., 2011).

Eggshell (ES) acts as a source of calcium oxide which contains 94% of calcium. So, this work is planned to synthesize of CaO/AC nanocomposites from eggshell and banana peels waste materials, which are common and cheap precursors by thermal decomposition and solid state reaction methods respectively and investigate the effect of CaO NPs and CaO/AC nanocomposite for degradation of Methylene blue dye.

1.3. Objectives of the Study

1.3.1. General objective

The general objective of this study is to synthesize, characterize, and evaluate photocatalytic efficiency of CaO nanoparticles (NPs), and CaO/activated carbon (AC) nanocomposites (NCs).

1.3.2. Specific objectives

- The synthesis involved the production of CaO nanoparticles via thermal decomposition, activation of carbon nanoparticles, and the preparation of CaO/AC-NCs through the solid-state reaction method.
- To characterize as synthesized CaO NPs, activation carbon NPs, and CaO/AC- composite using different analytical techniques such as XRD, UV-vis, FTIR, and SEM.
- To evaluate the effects of catalyst dosage, pH of the reaction media, and initial concentration of methylene blue dye on the degradation efficiency of the superiorly performing synthesized nanomaterial.

1.4. Significance of the Study

This study provides important information about the synthesis strategy CaO/AC nano-composite and their photocatalytic application. This research method prepares CaO from eggshell, using thermal decomposition method, AC from banana peels, using thermal decomposition method, and formation of CaO/AC nanocomposites by using solid state reaction method to be used for dye degradation. It demonstrates new method to clean and safe water resources for communities, improving public health and well-being. .

1.5. Scope of the Study

In this work CaO/AC nanocomposites was synthesized through solid state reaction method. The synthesized samples was characterized by UV-Visible spectroscopy (UV-Visible), Fourier transform infrared spectroscopy (FT-IR), X-ray diffraction (XRD), scanning electron microscopy (SEM), and its application for methylene blue dye degradation.

2. LITERATURE REVIEW

2.1. Water Pollution

Water pollution occurs when harmful substances, such as chemicals, pollutants, or microorganisms, contaminate water bodies like rivers, lakes, oceans, and groundwater. The main causes of it are sewage discharge, oil spills, industrial activity, runoff from agriculture, and incorrect waste disposal. The health of humans, ecosystems, and aquatic life can all suffer greatly from water pollution (Fraser *et al*., 2006). Water quality is influenced by many factors like precipitation, climate, soil type, vegetation, geology, ground water and human activities. The biggest danger to the quality of the water comes from industrial and municipal point sources. Water quality is also impacted by mining, urban development, and agriculture(Gikas & Tchobanoglous, 2009). Sediments, poisonous pollutants, and nutrients are additional components of non-point source pollution (Taiwo Adewale M, 2011).

Point source pollution is the term used to describe pollution in water that has a known source or t hat is entering the water from an identifiable source, such as a storm drain, sewage treatment pla nt, ditch, or pipe industry. It is distinguishable from additional sources of pollution. Non-point source pollution occurs when the source of water pollution is unknown or does not originate from a single, distinct source. It is extremely difficult to control and can originate from a variety of sources, including industrial waste, fertilizers, and pesticides (FN & MF, 2017).

Water pollution is the presence of excessive amounts of a hazard (pollutants) in water in such a way that it is no long suitable for drinking, bathing, cooking or other use. Contaminants released from industries and agricultural activity have become the main source, which affects most of the water bodies in the ecological system(Taiwo Adewale M, 2011). Organic dyes are one of the major pollutants released into wastewaters from textile and other industrial processes. About 10–20% of total dye products in the world is lost in textile wastes during the manufacturing process and released as effluents into the green environment.

Contaminated water effluents before discharging into the water bodies should be treated well to avoid such fate of water crisis. Several Figure 1.1 such as adsorption, membrane filtration, reverse osmosis, electrolysis, photo-catalysis, ion-exchange, desalination, flocculation, and biological precipitation have been implemented for wastewater treatment before discharge it into

the water mainstreams. Each method exhibits some advantages and disadvantages, including the generation of secondary waste. Photocatalytic treatment is one of the best and effective approaches to clean the water economically using renewable sources and semiconductor material.

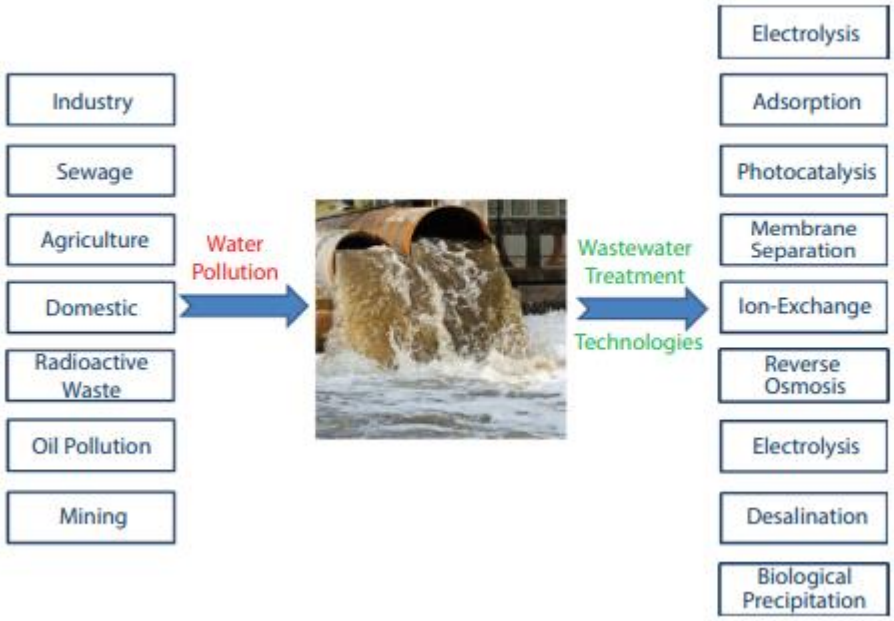

Figure 1. 1 Various sources of water pollution along with different technologies to clean the wastewater(Gusain *et al*., 2020).

2.1.1. Methylene blue dye (MB)

Methylene blue dye is known as methyl thioninium chloride. It is a basic cationic dye with the molecular formula $C_{16}H_{18}N_3SCl$ with a molecular mass of 319.87g/mol. It's IUPAC Name 3, 7-bis (dimethyl amino)-phenothiazin-5-ium-chloride. This dye gives a net positive charge when introducing with an aqueous solution because of the presence of chemical groups like amine or sulfur. At room temperature, methylene blue is solid, odorless, dark green powder and gives a blue solution when dissolved in water(Laysandra *et al*., 2017).

This dye is used in several applications like the coating and coloring of paper, hair, cotton, and wool; it is also used as an indicator of oxidation-reduction and as a disinfectant, besides its many other medical usages in medicine, in pharmaceutical formulations, in pesticide production, and varnish(Hamad & Idrus, 2022).

2.1.2. Application of Methylene Blue

MB is a desirable molecule having a range of qualities that make it helpful for biological applications. It is also an efficient medicinal drug that treats Barrett's oesophagus, anemia, and malaria. MB was the first synthetic antimalarial to be employed against all forms of malaria in the late 19th and early 20th century. It also has the ability to sensitize the body to chloroquine(Schirmer *et al*., 2003). The photodynamic therapy of cancer is being treated with MB dye (Mashkoor & Nasar, 2020). It is frequently used to photosensitize plasma for the photodynamic inactivation of RNA viruses, such as the hepatitis B, hepatitis C, and HIV viruses(Saha *et al*., 2018). According to recent research, MB could potentially prevent Alzheimer's disease and boost memory (Levine, 2020).

2.2. Source of dye pollutant

Water treatment operation is quested for many decades due to the contamination of water from chemicals, plastics, sewage wastes and microbial contaminants. As a result of industrialization, hazardous chemical products and antibiotics are widely used (Tan *et al*., 2021). Chemical wastes pose a serious risk since it takes a long time to recover water from them. A dye is one of the primary chemical wastes. Because they can be used on cotton, paper, leather, wool, and silk, dyes have a wide range of applications. The textile industry was their principal application(Hugo, 1995). One kilogram of textile requires about 200 liters of water to produce, and each textile mill uses more than 1.6 million liters of water every day. In addition, specific dyes are employed as markers. Using dyes offers many benefits to the paper, printing, pharmaceutical, tannery, and pulp industries. A significant amount of naturally occurring water resources are contaminated by organic dye pollutants that are produced by industries(Vishnu *et al*., 2020).

These pollutants prevail in the water for an extended period since the high resistance to heat and photo stability, which prevents biodegradation and has an impact on aquatic systems. Effective removal of dyes is a complex problem for chemical engineers because this process is neither economical nor efficient (Liu, 2020). Water containing dyes is highly undesirable due to its color and hardness. The toxic nature is due to the presence of carcinogens such as naphthalene, benzamine, and other aromatic compounds. Mordants are compounds used to fix dyes to fabrics and are highly toxic, making water toxic. Only 80% of the dye remains intact on the fabric while the rest is washed away. Synthetic dyes from the textile industry harm aquatic life due to their

micro toxicity. These synthetic dyes are also used in leather tanning, paper making, food technology, agricultural research, light collection arrays, photochemical cells, and hair dyes. Chemical dye classes used industrially are azo, anthraquinone, sulfur, indigoid, triphenylmethyl (trityl), and phthalocyanine derivatives. Azo dyes are the most commonly used in many industries(Vishnu *et al*., 2020).

2.2.1. Dyes in textile industry

The textile industry has been one of the major polluters of surface and ground water resources because it uses as many as 8,000 chemicals and huge amount of water and (54%) releases the highest amount of dye effluent, contributing to more than half of the existing dye effluents seen in the environment around the world. Several reports suggest that an average sized textile industry consumes about 1.6 million liters of water per day for the production of about 8,000 kg of fabric (Vishnu *et al.*, 2020). The dyeing industry (21%), paper and pulp industry (10%), tannery and paint industry (8%) and the dye manufacturing industry (7%) too are known to produce high amounts of dye effluents from various associated processes. The exact amount of dye effluents ejected by each industry into the environment is unknown but it can be said that the number is quite large to result as a significant environmental issue (Todd, 2015).

2.3. Methods of dye Removal

Furthermore, the cost associated with dye removal or remediation technologies is also a key factor. Ideally, a dye removal method should be capable of rapidly removing large quantities of dyes from wastewater without generating secondary pollution and cheaper. Technologies for dye removal can be divided into three categories: biological (fungal decolorazation, microbial decolorization, adsorption by living or dead microbial biomass, and anaerobic bioremediation), chemical (advanced oxidation processes (AOPs), electrochemical process, and coagulation or flocculation) and physical methods (adsorption, membrane filtration, ion exchange, electro-kinetic coagulation (Dassanayake *et al*., 2021).

2.3.1. Biological treatment methods

Biological methods, i.e. degradation of dyes with the biological phenomenon such as bioremediation is a green technique to remove dye from textile effluent with minimum cost and optimum operating time. Utilizing biologically based techniques has been effective in degrading textile industry wastewater. When compared to other methods, biological degradation, or

bioremediation, is more environmentally friendly, economically viable, and produces less sludge. Because of the breakage of the link (i.e., chromophoric group), it induces the degradation of synthetic dyes to a somewhat less hazardous inorganic chemical and ultimately aids in color removal (Bhatia *et al*., 2017).

Before dye effluents are released into the environment, a combination of aerobic and anaerobic processes is carried out, commonly referred to as the conventional method(Moradihamedani, 2022). The primary reasons this technique was selected as the standard for dye removal were its low cost and ease of use. In fact, colored water is still present in the environment because this treatment is unable to totally eliminate dangerous particles from wastewater containing textile dyes. The traditional method does not render the water toxic or dye-free, even though it does address the chemical oxygen demand found in the wastewater. In addition to this technique, other traditional biological dye removal methods include pure and mixed cultures, fungal cultures, enzyme and algae degradation, adsorption by microbial biomass, and degradation by enzymes. Since this method deals with living things, its major disadvantage is its growth rate. System instability is common in biological dye removal processes as predicting its growth rate and reactions can be tricky at times (Todd, 2015).

2.3.2 Chemical treatment method

Chemical dye removal techniques successfully remove dyes from wastewater by utilizing chemical principles. Advanced oxidation processes, electrochemical destruction, Fenton reactions, oxidation, ozonation, photochemical processes, and ultraviolet irradiation are important examples of conventional techniques. When synthesizing nanomaterial and using them in photo catalysis, these techniques have several benefits (Ismail & Sakai, 2022). The great efficiency of these synthetic materials in degrading pollutants under light irradiation is attributed to their increased surface features and compositions. Chemical processes also facilitate capability, which makes it possible to produce nanomaterial in bigger numbers appropriate for industrial use (Robinson *et al*., 2001). Chemical approaches are a viable route for the advancement of water treatment and environmental remediation technologies because of their efficiency and scalability(Azbar et al., 2004): (Todd, 2015).

2.3.3. Physical treatment methods

Physical dye removal methods are usually straightforward methods commonly accomplished by the mass transfer mechanism. Conventional physical dye removal methods are adsorption, coagulation or flocculation, ion exchange, irradiation, membrane filtration, nano filtration or ultra-filtration and reverse osmosis (Nawaz & Ahsan, 2014). Among the three methods (biological, chemical and physical), branches of physical dye removal are the most commonly used methods. These methods are often chosen for its simplicity and efficiency. By far, this method requires the least amount of chemicals compared to the biological or chemical dye removal methods. This method does not deal with living organisms hence is considered to be more predictable than the other two dye removal methods (Todd, 2015).

2.4. Photo catalysis

Through the process of photocatalytic degradation, light energy typically from ultraviolet (UV) radiation is used to start chemical reactions that convert pollutants into harmless substances. Reactive oxygen species (ROS), which are extremely reactive substances produced by materials that can absorb light, are used in this process (Xie *et al.*, 2023). Heterogeneous photo catalysis is an advanced oxidation process (AOP) that is used to photo-degrade toxic compounds in wastewater without producing any secondary waste. Photo catalysis, which is fueled by semiconductor materials that function as photo catalysts with the appropriate band gaps under light irradiation, is the method used to degrade toxic chemicals (Das *et al*., 1999). A semiconductor substance known as a photo catalyst is exposed to light and, following photon absorption, generates species that are catalytically active. The energy of the photon should match or exceed the band gap of the photo catalyst. The goal of photon absorption is to produce charge carriers (such electrons and holes) that participate in redox reactions to degrade dangerous substances that have accumulated on the photo catalyst's surface. This reaction produces hydroxyl radicals (•OH), which operate as strong oxidants and degrade dangerous substances. The positive pores created facilitate the oxidation of contaminants (Vanthana Sree *et al*., 2020).

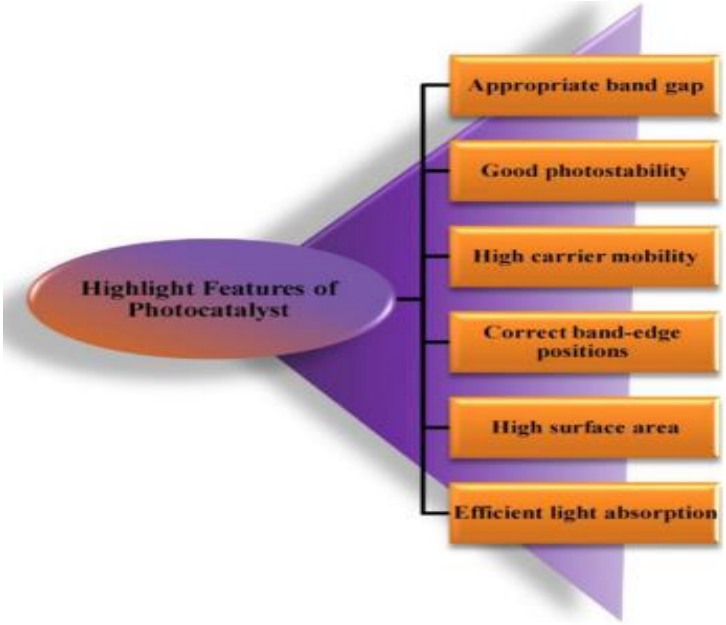

Figure 2. 1 Characteristic features of good quality photo-catalyst (Tomar *et al*., 2020).

2.4.1. Photo-catalysis mechanism

In a heterogeneous photo-catalysis process, the photo-catalyst absorbs light with the right amount of energy when illuminated, which excites the electrons in the valence band to move into the conduction band and initiate the photochemical reaction. Following the absorption of light by a photo-catalyst, four major steps occur during photocatalytic reactions: (i) formation of charge carriers over the VB and CB, (ii) recombination of the photo-generated e/h^+ pairs, (iii) trapping of the e/h^+ pairs in redox reactions, and finally (iv) the main photocatalytic reactions such as pollutant degradation. The incidence of light with the same or higher energy than the energy gap (Eg) of the used semiconductor drives electrons from the VB to the CB, leaving positive holes in the VB and thus creating e/h^+ pairs in the first step. Nonetheless, the photoinduced e/h^+ combinations are not energetically stable, and some of them recombinate, neutralizing each other and emitting heat. The second stage, whether on the surface or in the bulk, significantly lowers the effectiveness of photocatalytic reactions. In the third phase, photo induced holes and electrons transfer to the surface of the photo-catalyst and react with the adsorbed species on the surface, resulting in the creation of certain active species (e.g., O_2, OH) capable of launching a series of redox reactions. Finally, depending on the type of photocatalytic activity, reduction and oxidation reactions occur over the CB and VB of the photo-catalyst in the last phase (Pirhashemi *et al.,* 2018).

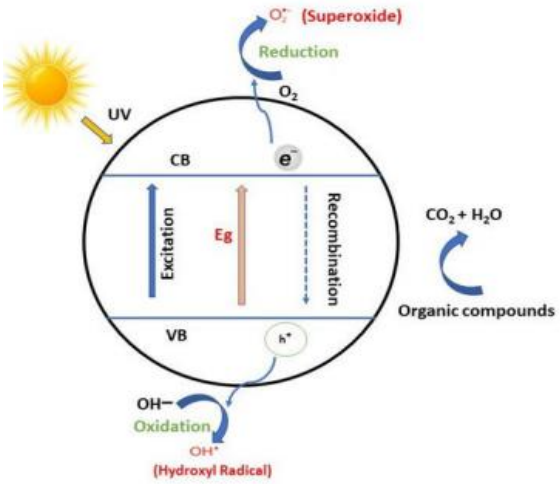

Figure 2. 2 General mechanism of the photocatalysis(Gusain *et al*., 2020)

Once the electron gets the sufficient energy (equivalent to band gap energy), it jumps from valence band to conduction band with the formation of hole in valence band. Electron reacts with the dissolved oxygen (O_2) in aqueous solution which also acts as the electron scavenger results in the formation active free radicals •OH, O_2^- , etc. Simultaneously, holes was get electron from electron donors (H_2O), resulting in OH free radicals formation. After the free radical formation, dye molecules were attacked by active species (•OH, O_2^- etc.) and ended in the de-coloration and opening-ring reactions.

$Dye + hv \rightarrow dye^*$ (Absorption of photons and excitation of dye molecules)

$hv + CaO \rightarrow e^-(CB) + H^*(VB)$ (Electron-Hole pair formation)

$e^-(CB) + O_2 \rightarrow \bullet O_2^-$ (Oxygen ion-sorption)

$2O_2^- + 2H_2O \rightarrow H_2O_2 + 2OH^- + O_2$ ($\bullet O^-$ Neutralization by protons)

$H_2O_2 + e^-(CB) \rightarrow {}^-OH + \bullet OH$ (Decomposition of H_2O_2 and •OH formation)

$h^+ + H_2O \rightarrow H^+ + \bullet OH$ (water splitting by photo-hole to produce •OH radicals)

$\bullet OH / \bullet O_2^- + dye \rightarrow$ Dye degradation (Electrophilic attack on Dye molecules)

During the degradation reaction, photo-holes remain inactive in the initial step due to the cationic nature of reactant(Vanthana Sree *et al*., 2020).

2.5. CaO as a photo-catalysis

Calcium oxide (CaO as quicklime) is a white, caustic, alkaline, crystalline powder made from the thermal decomposition of limestone or shells containing calcium carbonate ($CaCO_3$). Chemically synthesized CaO is used as catalyst in many industries in the form of toxic waste remediation agent, bactericide, adsorbent and binder in paints etc(Annam *et al*.,2016, Tangboriboon *et al*.,2012, Niju *et al*., 2014). Chemically synthesized CaO is used as photo-catalyst in degradation of organic dyes such as methylene blue (Rameshwar *et al*., 20) Congo red, Malachite green, Indicocarmine (Devarahosahalli Veeranna et al., 2014)Violet GL2B (Gopalappa *et al*., 2012), crystal violet (Sawant *et al*., 2016).

Eggshell(ES) also acts as a source of calcium oxide which contains calcium carbonate(Vanthana Sree *et al*., 2020)(Habte *et al*., n.d.). Egg is an important nutrient source for humans as it contains excess of protein, which is consumed up to million metric tons per year. These ES derived CaO NPs have been utilized in many fields namely biodiesel production(Boey *et al*., 2011), adsorption of pollutants and heavy metals(Lin *et al*., 2005), dielectrics, catalysts, biomaterials, fuel cell applications and fillers. CaO synthesis is a simple and easy process which does not need any solvent or chemicals for processing and results in eco-friendly and sustained material. One of the most common solid catalysts for the trans-esterification reaction of various feed stocks to biodiesel is calcium oxide (CaO), which has already shown to be a very effective catalyst for the synthesis of biodiesel. CaO is inexpensive, readily available, noncorrosive, environmentally friendly, easy to handle, and has a low solubility and high basicity.

Several researchers are interested in studying CaO more in order to enhance its overall qualities because of all these benefits. CaO can be made into a nano-form to increase its specific surface area and thereby boost its catalytic activity nano sized CaO–based catalysts and their application in the biodiesel production. Various forms of nano–sized CaO–based catalysts have been employed in the biodiesel production like neat, doped and loaded CaO as well as waste material containing CaO (Banković-Ilić *et al*., 2017).

2.6. Activated Carbon

The porous solid known as activated carbon (AC) has 85–95% carbon in it(Jha & Maharjan, 2022). By heating carbon-containing materials to a high temperature, AC can be produced. Pores may have the ability to adsorb carbon. In the food industry, bulky-surface AC has been used as a color remover, reliever, deodorizer, and purifying agent, among other uses. It is also frequently utilized in the process of purifying water, which includes treating wastewater as well as producing drinking water. The advantages of AC prepared using agricultural by-products offered an effective, inexpensive replacement for non-renewable coal based granular AC, which has similar or better adsorption efficiency(Viena *et al*., 2018).

2.7. Synthesis of Nanomaterial's

There are two main approaches for the synthesis of nanomaterial's: top-down approaches and bottom-up approaches. The term "top-down" refers to reduction by attrition and different conventional methods of comminution, which are the traditional methods of producing fine particles. In recent years, "bottom-up" production approaches have become more and more popular. The term "bottom-up approach" describes the process of either building a substance from the bottom up, atom by atom, molecule by molecule, or cluster-by-cluster (Tulinski & Jurczyk, 2017).

Top-down approaches have a number of significant drawbacks, including the inability to regulate the size, morphology, and other structural characteristics of the created particles. The form, size, and morphology of the resulting particles can be significantly controlled using bottom-up approaches, which begin at the molecular level. Because the structural properties of the resulting products are delicately controlled, bottom-up techniques are more common and widely used(Xia *et al*., 2009). Reagents include growth inhibitors, ligands, and surfactants that can help control

the growth process of nanostructures in the bottom-up approach (Siddique & Gonzalez-cortes, 2022).

Top-down approaches include mechanical milling, laser ablation, sputtering, and electro-explosion. While bottom-up approaches include Chemical Vapor Deposition, green synthesis, sol-gel, co-precipitation, solution combustion etc (Yec & Zeng, 2014).

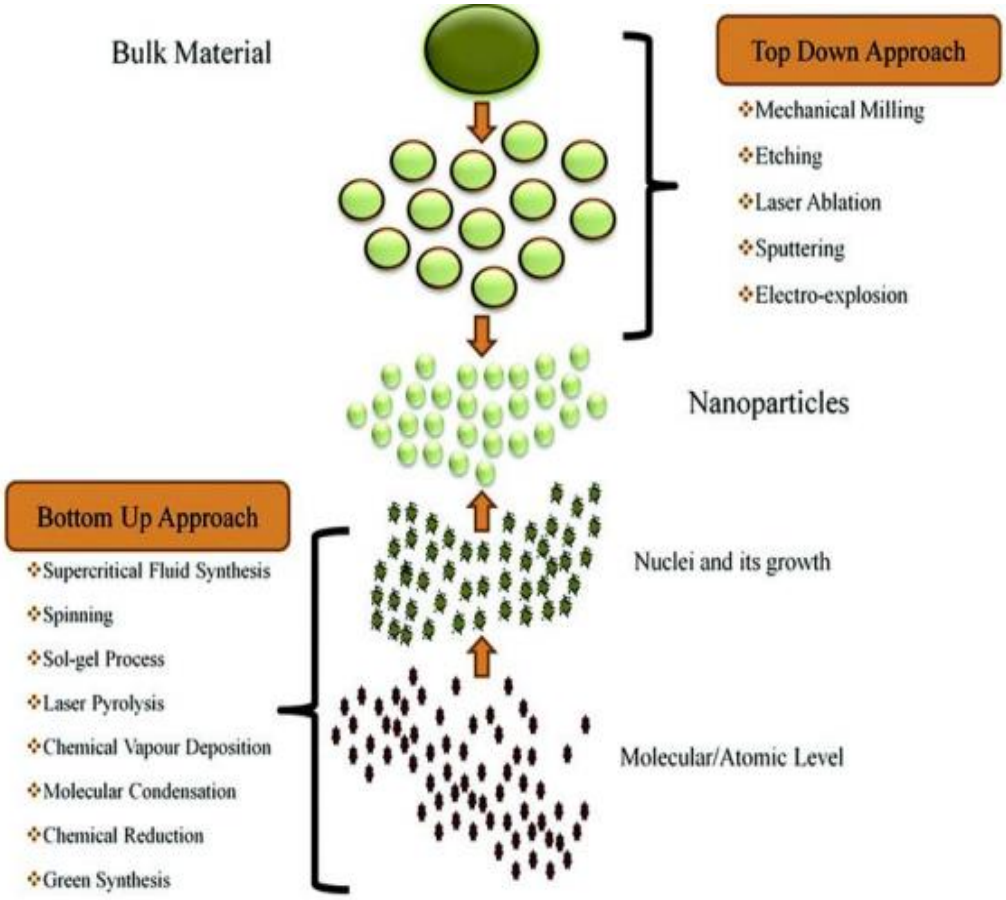

Figure 2. 3 Top-down and bottom-up methods for synthesizing nanomaterials (Bhagwat *et al*., 2019)**.**

2.7.1 Fundamental of the bottom-up synthesis approach

Due to the essential differences between the bulk equivalents and the nanoscale-sized materials, attention has been generated in numerous disciplines. The current development is the bottom-up synthesis of nanocrystals with precise shape, size, and structure by comprehending the precursor breakdown, nucleation, and growth processes under challenging external and interior conditions(Grzelczak *et al*., 2010). Controlling the nucleation and growth development processes

are crucial procedures before the formation of nanocrystals. The first model to explain precursor decomposition and reduction, nucleation, development into seeds, and finally growth into nanocrystals in solution was La Mer's group theory (Abebe *et al*., 2021). In the 1950, La Mer and his colleagues proposed the idea of burst nucleation, transferring the concept of CNT to NP syntheses. Their investigation into diverse oil aerosols 16 and sulfur hydrosols led to the development of the ground-breaking idea. In the burst nucleation process, homogeneous nucleation causes the simultaneous generation of many nuclei, which then expand without further nucleation. That concept of NP formation's fundamental principle is the distinction between nucleation and growth. One interpretation is that a homogeneous phase and a heterogeneous phase are separated(Sawant *et al.*, 2016).

3. MATERIALS AND METHODS

3.1 Chemical and Reagents

The chemicals and reagents were analytical grade and used without further purification. Hydrochloric acid (HCl 99%), Sodium hydroxide (NaOH 98%), Ethanol (ethyl alcohol 95%), and methylene blue ($C_{16}H_{18}ClN_3S$) (Sigma Aldrich) and distilled water was used throughout the experiment.

3.2 Preparation of CaO Nanoparticles

A precursor (Eggshell) waste was collected and first washed completely with tap water to remove dust, impurities, and organic matters adhered on the surface of the eggshells, followed by another cleaned with distilled water several times. Then the efficiently washed eggshells were oven-dried at 130◦C for 3hr to remove water. The dried eggshells were ground by a grinder machine to get the fine powder(Kasirajan *et al*., 2022). 50.00 g of cleaned and ground eggshell powder were placed in a crucible and heated to 800^0C in a furnace. After calcining In order to prevent hydrolysis, the sample crucibles were removed from the muffle furnace and allowed to cool in the air for ten to twenty minutes, show in Figure 3.1.

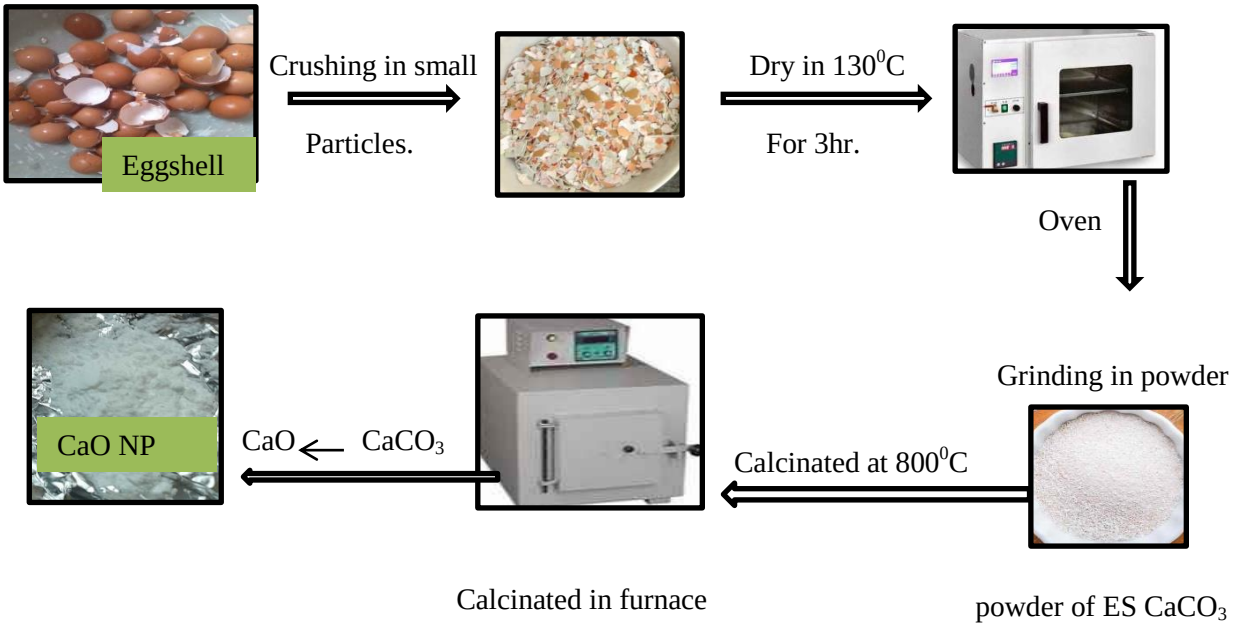

Figure 3. 1 Synthesis of CaO from Eggshell (ES)

Fresh raw materials like calcite must be pre-treated at a high temperature in order to undergo thermal decomposition and to increase the quantity of active sites on the surface of catalyst particles. The availability of basic sites for catalysis is generally a determinant of the catalyst's efficiency. The chemisorption of carbon dioxide and water on the basic sites of CaO in air reduces the amount of active sites available for catalysis. The calcination conditions, particularly temperature, determine the type of basic sites on the surface of solid particles. Raising the temperature of calcination affects both the readjustment of catalyst atoms on the particle surface and the desorption of molecules, which obstructs active sites(Banković-Ilić *et al*., 2017).

3.3 Preparation of Activated Carbon

The raw banana peel was collected from local market. To get rid of any last bits of dust, it was cleaned with distilled water. To hasten the drying process, the peel's size was lowered from 1 to 2 cm. Following a three-hour oven bake at 105^0 C to eliminate any remaining moisture, all of the leaking water was drying in the oven (Nadew *et al*., 2023). The dried peels were carbonized in the furnace for 1.5 hours at 400 ^{0}C. Small-scale carbon grinding was done using a mortar and pestle. It was then filtered, extensively cleaned with aquadest, and heated for two hours at 200°C (Viena *et al*., 2018).

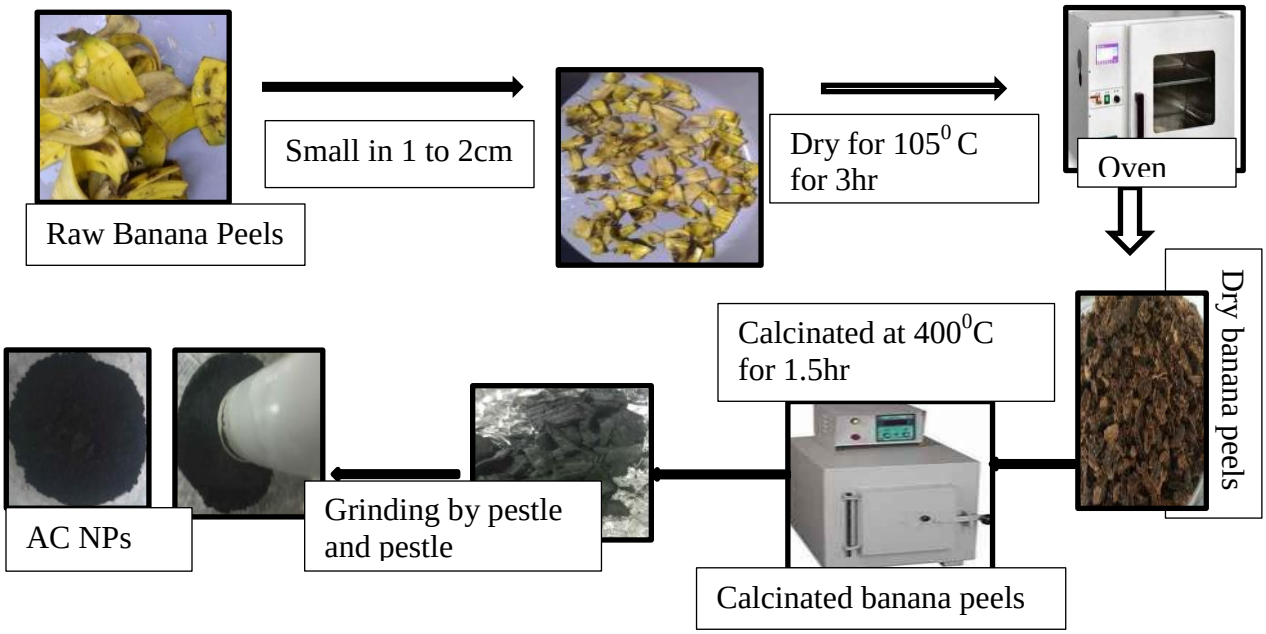

Figure 3.2 Synthesis of banana peels waste

3.4 Synthesis of CaO/AC Nanocomposites

Composites were fabricated by varying the mass of activated carbon and CaO. A total of 10g of the composites were made using the following compositions: 100% CaO (sample A), 50% CaO and 50% activated carbon (sample B), 30% CaO and 70% CaO (sample C), and 70% CaO and 30% activated carbon (sample D). After being left to stand at room temperature for 48 hours, the composites were calcined for two hours at 400°C in a furnace (Science, 2021).

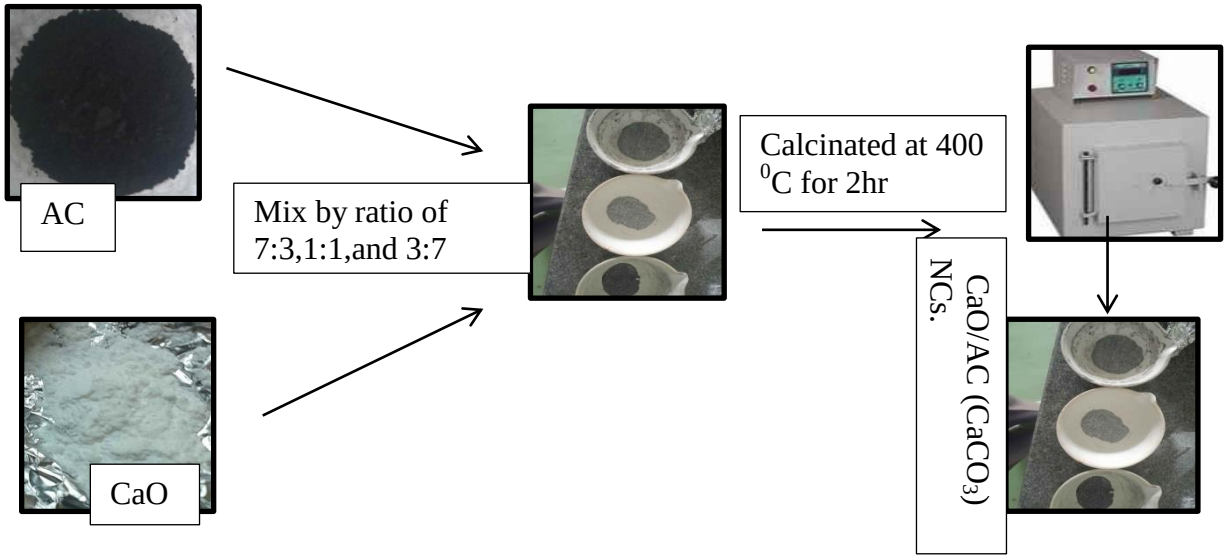

Figure 3. 1 Synthesis of CaO/AC ($CaCO_3$) composite nanoparticles

3.5 Photocatalytic dye Degradation Studies

The photocatalytic experiments were conducted by taking the appropriate amount (in ppm) of target dye/s in an aqueous solution with the weight amount of the synthesized NPs and NCs catalysts. CaO and CaO/AC nano powders were photo catalytically tested with methylene blue (MB) dye under UV visible. The photocatalytic experiments were performed as a function of the irradiation time, catalyst mass, pH value, and concentration methyl blue of the photo-catalyst.

The degradation experiment was conducted either in the laboratory developed glass reactor or a reactor purchased/available. The samples were irradiated directly by focusing light into the reaction mixture at a standard distance from the reactor. Magnetic stirring was applied to continuously mix the solution. The temperature of the overall reactor was controlled either using water circulation or an electric fan(Chong *et al*., 2010). At twenty (20) minutes intervals, the dye concentration was measured by UV-vis spectrophotometer, and the degradation efficiency in

percent was calculated using Equation 1.The pseudo-first-order kinetic equation (Equation 2) was used to study reaction dynamics (Abebe *et al.*, 2021).

$$\text{Degradation yield}(\%) = \frac{Co-Ce}{Co} \text{x}100 \ldots\ldots\ldots\ldots(1)$$

$$\text{Pseudo- first-order kinetics; } \log \frac{C}{Co} = -kt \ldots\ldots(2)$$

3.5.1 Effect of the photo catalyst mass (Dosage)

The effects of the photo catalyst mass 10mg and 30mg on the photodegradation of 10 ppm MB dye were tested at pH 12 in 50 mL MB dye solutions for 0-80 minutes (Saeed *et al*., 2022).

3.5.2. Effect of the pH value

0.1 M NaOH and 0.1 M HCl were used to control the pH value of 50 mL MB dye solutions with an initial dye concentration of 10 ppm. The effect of the pH value at 5 and 12 on the photo degradation of the prepared MB solutions was studied using 30mg of the photo-catalyst(Ali *et al.*, 2024).

3.5.3. Effect of Dye Concentration

The photo-catalytic degradation rate of a certain dye or pollutant depends on its concentration, nature and on the presence of other existing compounds in the water matrix. Kumar and Pandey (Kumar, 2017) reported that the photocatalytic degradation processes are contributed by the dyes which adsorbed on the catalyst surface but not in the bulk of the solution. They stated that initial concentration of dye played an important role in the photocatalytic degradation efficiency and generally favored at low dye concentration.

3.6 Characterization

3.6.1 X-ray Diffraction (XRD)

X-ray diffractometer was used to perform X-ray Diffraction (XRD) analysis of the catalysts in the range from 5 to 80. The crystallite size of sample was estimated using Debye Scherrer‟s formula based XRD spectrum result(Chong *et al*., 2010). Debye Scherrer‟s formula to be estimated

$$D = \frac{k\lambda}{\beta \cos \theta}$$

Where, D……. average Crystallite size in nm. λ = 1.54 A^0 ….wavelength of the X – ray source

β Full Width at Half Maximum (FWHM) of a peak

θ …angle of diffraction of X-ray. K the shape factor.

3.6.2. Scanning Electron Microscopy (SEM)

The surface morphology were characterized by scanning electron microscope (SEM). It provides detailed information about the microstructure of materials at a Nano scale level(Olivares-Marín *et al*., 2013).

3.6.3. Fourier Transform Infrared Spectroscopy (FT-IR)

The chemical functional groups of the catalysts were studied through the use of a Fourier transform infrared spectroscopy (FT-IR) analysis (Vertex 70 FTIR-FT Raman spectrometer) in a range of 4000-400 cm^{-1}.

FT-IR measured the sample's interaction with infrared light to determine its molecular makeup. It gave important details about the many kinds of chemical bonds in the sample, the functional groups that make up molecules, and the general structure of the molecules(Hadjiivanov, 2014).

3.6.4. Ultraviolet-Visible light

Analyzing the interaction between ultraviolet (UV) and visible light and a sample is possible via UV-visible spectroscopy. The electrical structure and concentration of the chromophore in the sample are both usefully disclosed. The interaction between UV and visible light and a sample is measured in UV-visible spectroscopy in order to ascertain the sample's transmittance or absorbance. Samples in the wavelength range of 200–800 nm was subjected to UV–Vis spectrum analysis.

3.7. Data Analysis

Origin Pro 8 software was used for the UV-Vis, XRD, and FTIR analyses that produced the data about the environmentally generated nanomaterial.

4. RESULTS AND DISCUSSION

The study presents a comprehensive characterization and application of CaO and its composite with activated carbon (AC) in the photocatalytic degradation of methyl blue in waste water. Techniques such as Thermogravometric Analysis (TGA), X-ray Diffraction (XRD), Fourier-transform Infrared Spectroscopy (FTIR), and Scanning Electron Microscopy(SEM) were employed to analyses the materials. The photocatalytic efficiency was assessed under varying conditions, including different dosages of the photo-catalyst, PH levels, and concentration of the dye. The results indicates that the CaO and CaO/AC composite ($CaCO_3$) effectively degrade methyl blue, with performance influenced by the operational parameters.

4.1. Thermal Analysis

TGA analysis was done to know the thermal stability, decomposition temperature, and decomposition phase occurring during heat treatment of synthesized samples. Figure 4.1 were established thermal stability and breakdown temperature of raw eggshell powder (RESP) between room temperature and 1000˚C. Three steps in the decomposition process were visible in the TGA curve. First, 1.5% of the weight was lost between 0˚C and 271˚C, which was probably caused by the dehydration and organic matter removal. A subsequent 3.4% weight loss took place between 271˚C and 616˚C. The breakdown of $CaCO_3$ occurred between 616˚ and 788˚C, which was the most significant disintegration and resulted in a high weight loss of 46.44%. The determined steps of decomposition, additional investigation could examine the impact of heating rates on RESP's behavior during decomposition. A more thorough understanding of the thermal behavior of materials formed from eggshells might be obtained by adjusting the heating rate during TGA analysis, which would provide insights into the kinetics of the decomposition processes.

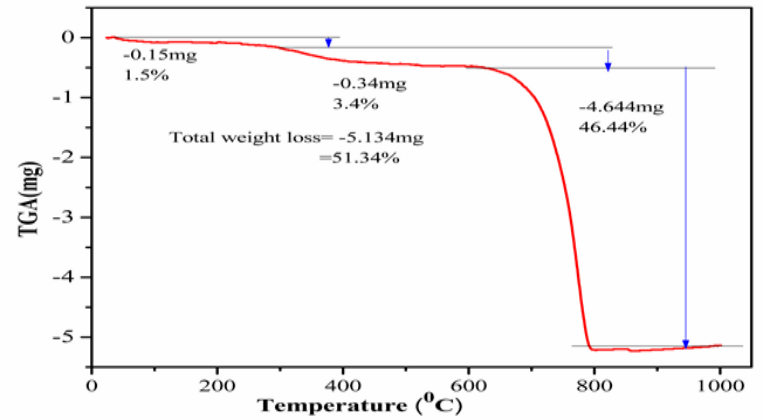

Figure 4. 1 The Graph of TGA analysis of raw eggshell powder**.**

CaO NPs had high thermal stability and purity. Therefore TG curve of the pure compounds shows the characteristics of the compounds(Kasirajan *et al*., 2022).

4.2 X-ray diffraction studies (XRD).

The peaks identified from the diffraction pattern corresponding to the CaO (based on JCPDS card # 48-1467) at 2θ of 32.39, 37.54, 54.09, 64.40, 67.60 and 79.79^0. These peaks are attributed to the growth alongside (111), (200), (220), (311), (222) and (400) planes. The material's crystalline structure is confirmed by the intense and narrow peaks in calcined eggshells. This indicates that the eggshells are fully crystallized during the calcination process. The cubic system of the CaO catalyst has a face-center lattice. The XRD-pattern obtained shows diffraction peaks obtained are characteristics of calcium oxide (CaO)(Islam *et al*. 2011).

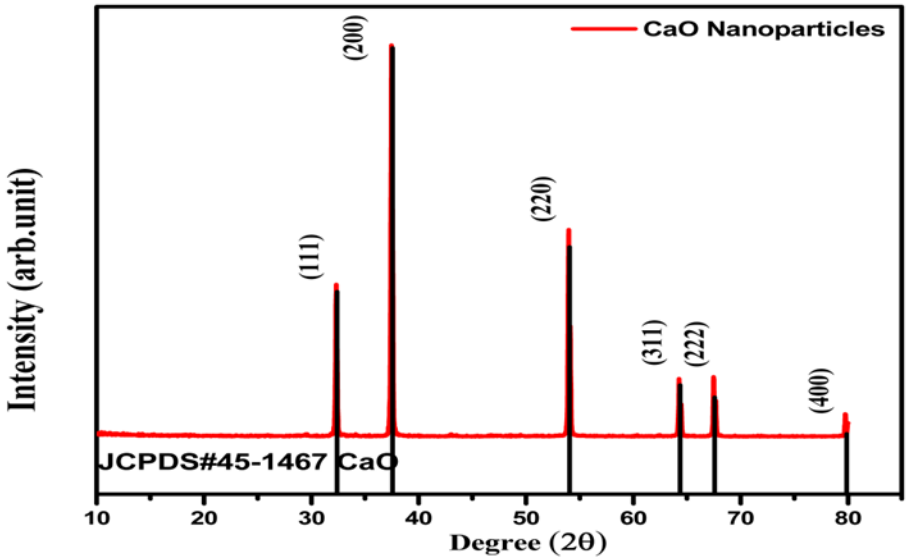

Figure 4. 2 XRD pattern of CaO calcinated at 800^0C.

The XRD patterns of activated banana peels formed by physical activation are shown in Figure 4.3. Sharp peaks were seen in the XRD profiles for calcinated banana peels, which suggested that the structure of the activated carbon had changed. It was verified that the 400^oC pyrolysis temperature of activated banana peels carbon caused thermal breakdown and the creation of additional crystalline carbon at 24.33, 28.39, and 31.347 degrees Celsius. Furthermore, there was evidence of residual amorphous carbon, as seen, for instance, at (10-23.97)º, indicating that some amorphous carbon remained and the pyrolysis reaction was not finished.

Detected in the activated carbon's structure, more research might be done to examine the possible ramifications of these discoveries. For example, looking at how these structural alterations affect how well activated carbon works in different applications, like cleaning water or contaminating methyl blue dye, Additionally, investigating the connection between the activated carbon's amorphous and crystallinity and its capacity for adsorption of various pollutants may provide insightful knowledge for enhancing the material's effectiveness in environmental restoration procedure (Lewoyehu, 2021).

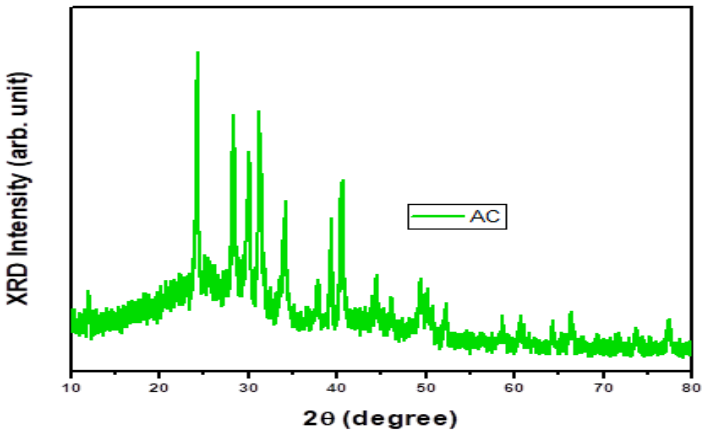

Figure 4. 3 Crystallize size analysis of activated carbon

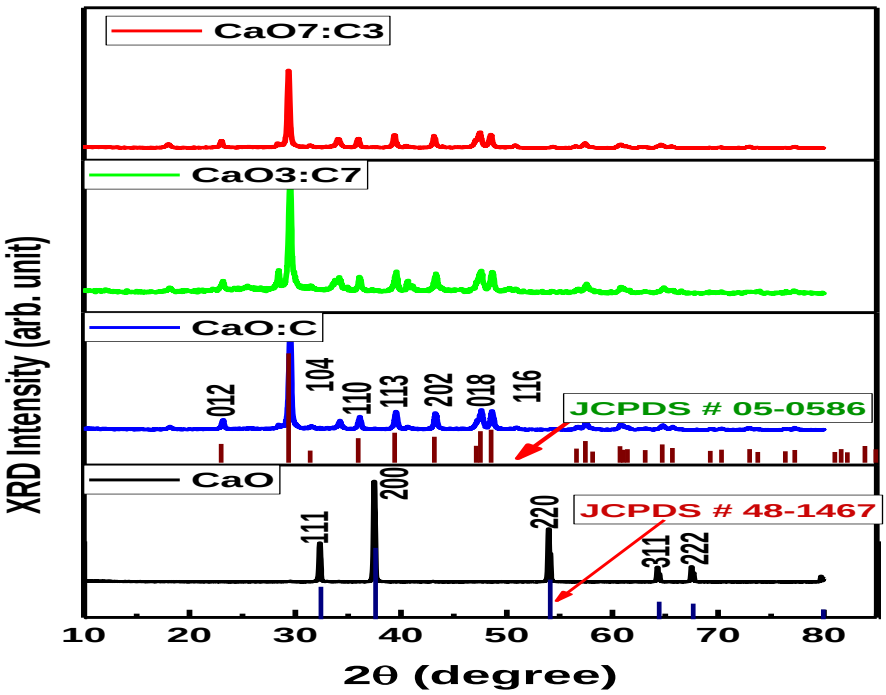

Figure 4. 4. XRD pattern of the composite CaO with activated carbon($CaCO_3$).

At 400°C, the combination of CaO and Activated Carbon undergoes a complete chemical reaction to form $CaCO_3$, rather than creating a CaO/AC composite. This transformation is confirmed through X-ray diffraction (XRD), a powerful technique for identifying crystalline phases in materials. Analysis of the synthesized sample revealed the formation of calcite, the

most stable and common form of $CaCO_3$, as evidenced by JCPDS card #05-0586. The key diffraction peaks for calcite appear at specific 2θ angles, notably at approximately 29.4°, 39.4°, 43.1°, 47.5°, and 48.5°. Each peak corresponds to distinct crystallographic planes such as (104), (110), (113), (202), and (118).

The pattern of the synthesized sample matches the JCPDS card for pure calcite with no additional peaks, indicating the absence of other phases or impurities. If extra peaks were present, they could suggest the existence of other $CaCO_3$ polymorphs like aragonite or vaterite, or other impurities. This finding confirms that a pure calcite phase forms in all combinations of CaO and Activated Carbon, with no evidence of a CaO/AC composite.

The DebyeeScherrer equation was used to calculate the crystallite sizes of CaO, AC and composite of CaO with AC. Table 4.1 shows crystallite size of these sample. The samples' estimated crystallite sizes shed important light on their structural properties and possible photocatalytic activity. The more apparent crystalline structure of CaO, as indicated by its greater crystallite size of 59.5 nm, may improve its stability and reactivity in photocatalytic processes. However, a more amorphous or disordered structure is suggested by activated carbon (AC) with a smaller crystallite size (26.30 nm), which have a larger surface area and increased potential for organic pollutant adsorption. The composite ratios of 3:7, 1:1, and 7:3 of CaO with AC as determined by XRD analysis showed that the average crystal sizes were, respectively, 25.62 nm, 29.48 nm, and 27.99 nm. These results imply that the crystalline structure of the resultant materials is influenced by the fluctuation in the composite ratios. In comparison to the other composites, the one with a 1:1 ratio had the highest average crystal size, suggesting a possibly more organized and compact structure. On the other hand, the composite with the 3:7 ratio showed the smallest average crystal size, indicating a crystalline structure that is finer and maybe more distributed. The 7:3 composite was halfway between these two extremes.

The characteristics and performance of the material are affected by larger crystal sizes, which frequently suggest slower reaction kinetics and a different surface area-to-volume ratio. Increased surface area and improved reactivity are typically the results of lower crystal sizes. When compared to the composite material, calcium oxide (CaO) showed a noticeably more porous and rough structure. When compared to the composite, this increased porosity led to a noticeably better breakdown efficiency in CaO, notably in calcium carbonate ($CaCO_3$). This

shows that CaO outperforms $CaCO_3$ in terms of degradation efficiency because of its rough and porous nature, which promotes accelerated degradation processes.

Table 4. 1 DebyeeScherrer calculation of CaO, AC and composite of CaO with AC ($CaCO_3$).

Type of sample	2 (deg)	FWHM	Average Crystallize size
CaO	37.4908	0.15000	59.53nm
	53.9874	0.14660	
	32.3406	0.15050	
AC	24.3319	0.26080	26.31nm
	31.3475	0.37960	
	28.3948	0.33520	
7:3 ratio	29.3897	0.26090	27.99nm
	47.4261	0.40930	
	39.3856	0.27270	
1:1 ratio	29.5316	0.27480	29.48nm
	48.6075	0.31730	
	39.5285	0.30470	
3:7 ratio	29.5238	0.31670	25.62nm
	39.5301	0.33470	
	48.6223	0.38110	

4.3. Morphological Study (SEM).

It is well established that photocatalytic behavior is highly influenced by the surface morphology of the photo-catalyst. The 10 µm magnification showed Figure 4.5. In figure 4.5a indicate that CaO is known for its porous nature, characterized by the presence of voids and channels within the crystal lattice. These pores provide increased surface area and facilitate the adsorption of gases and other substances. Porous and with a regular crystal structure, pure CaO offers a strong

foundation for photocatalytic processes. A sizable surface area is provided by the porous structure for reactant adsorption and catalytic activity. When exposed to light, CaO can help produce reactive oxygen species (ROS), which can accelerate the breakdown of the dye molecules in methyl blue.

In 3:7 ratio because activated carbon is included in this composite, an amorphous structure forms. The majority of activated carbon is disordered, and its crystal structure is not well defined. The composite might have a mix of amorphous activated carbon matrix and irregularly shaped CaO particles, which would lead to a heterogeneous morphology with distributed active sites and make it easier for methyl blue molecules to adsorb.

In 1:1 ratio combination of crystalline and amorphous structures may be seen in the composite morphology when the ratio of CaO to AC is equal. Throughout the amorphous activated carbon matrix, there are scattered regular-shaped CaO crystals. This combination strikes a balance between the high surface area of activated carbon and the well-defined structure of CaO, which may improve the composite's efficiency in the photocatalytic degradation of methyl blue.

In 7:3 ratio Because of the increased CaO content in this composite, CaO crystals contained in an amorphous activated carbon matrix may dominate the morphology. In comparison to the other composites, the presence of more CaO crystals results in a more organized shape while maintaining the porous nature of CaO. But activated carbon's amorphous character endures, adding to the composite's overall variability.

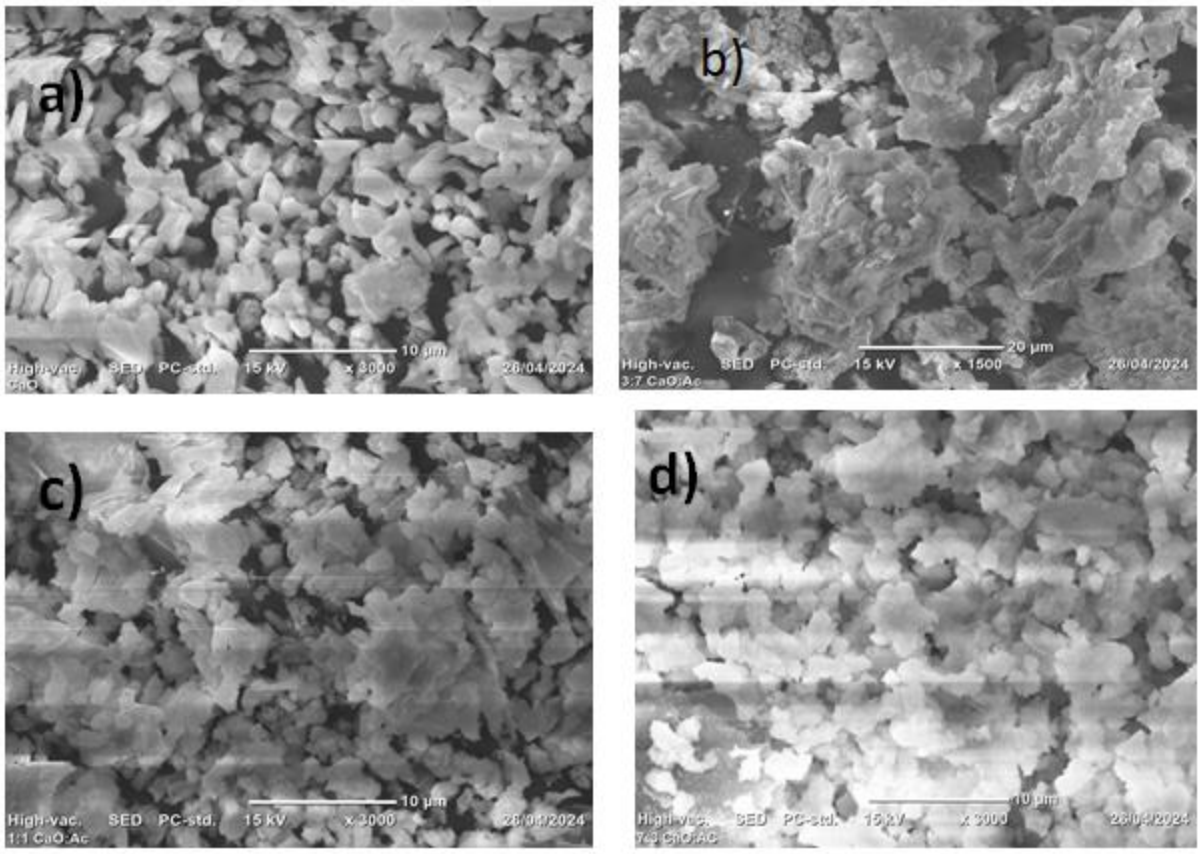

Figure 4. 5. SEM analysis of CaO and composite of CaO with AC ($CaCO_3$) a) CaO, b) 3:7 CaO with AC, c) 1:1CaO with AC, d) 7:3 CaO with AC

4.4 Fourier Transform Infrared (FTIR) spectra analysis

Significant peaks in the wavenumber range of 4000-400 cm^{-1} are revealed by the FT-IR data for CaO and CaO/AC photo catalysts shown in Fig.4.7, offering important information on their structural properties. Peaks were found in pure CaO with wavenumbers of 3640.44,3644.00, 3006.02, 2648.28, 2027.54, 1417.25, 1413.00,1218.38, 1140.00,1138.63, 875.09, and 446.16 cm^{-1}. 3640.44 cm^{-1} and 3644.00 cm^{-1} these peaks show that the surface of CaO has hydroxyl groups (OH). The surface of the photo-catalyst can serve as an active location for the adsorption of MB dye molecules by hydroxyl groups. 3006.02 cm^{-1} peak indicates the possibility of organic contaminants or leftovers from the precursor eggshell. These residues may affect the photo-catalyst's overall performance even though they are not directly related to photocatalytic activity. 2648.28 cm^{-1} and 2027.54 cm^{-1} show that carbonate species have been adsorbed onto the CaO surface. During photo-catalysis, carbonate ions (CO_3^{2-}) can aid in the production of reactive oxygen species (ROS), which accelerates the breakdown of MB dye molecules. The remaining

peaks correspond to extra carbonate vibrational modes as well as potential additional contaminants or functional groups. They all have an impact on the surface characteristics and reactivity of the CaO photo-catalyst, even if their individual contributions to photo-catalysis may differ(Meshkatalsadat *et al*., 2022).

According to prior research on commercial CaO, the stretching vibration of O-H is responsible for the absorption band between 2600 and 3600 cm^{-1}. The spectrum broad absorption peaks at around 3400–3650 cm^{-1}, indicates the presence of carboxylic acid and amino groups. The absorption band at 2900-2970cm^{-1} could be assigned to asymmetric vibration of –CH. The stretching vibration bands 1600-1650 cm^{-1} is due to asymmetric stretching of the carboxylic C=O double bond. A band at 1365-1400cm^{-1} is of phenolic –OH and –C=O stretching of carboxylates(Bathla *et al*., 2019).

The FTIR spectra of the composite CaO with AC ($CaCO_3$) exhibited a more complex nature, with peaks at wavenumbers of 3641.38, 3343.47, 2511.80, 2014.84, 1978.34, 1794.95, 1399.40, 1060.53, 873.22, 748.89, 710.52, 478.08, and 431.34 cm^{-1} for the 7:3 ratio. 3641.38 cm^{-1} and 3343.47 cm^{-1} OH stretching vibrational. 2511.80 cm^{-1} relate to the component of activated carbon's aromatic C=C stretching vibrations. Activated carbon is not directly engaged in the photocatalytic process, but it can increase the composite's total adsorption capacity, which improves the effectiveness of dye removal. Within the composite, the other peaks stand for different functional groups and vibrational modes. Additional OH stretching vibrations, C-H bending vibrations, and other chemical vibrations might be among them. The surface characteristics and reactivity of the composite photo-catalyst are influenced by them all, even if their individual contributions to photo-catalysis may differ(Soroush *et al*., 2022).

A strong and broad peak in the range of 1300 to 1500 cm^{-1} also suggested bending vibration and asymmetric stretching of the $CaCO_3$ complex, as shown by a distinctive peak at 518 cm^{-1}(Sahadat Hossain *et al*., 2023). Similar peaks were observed in the FTIR spectra for the 3:7 and 1:1 ratios of CaO: AC composites, with wavenumbers of 3360.30, 2510.69, 1794.86, 1402.69, 1068.21, 872.33, 710.732, 644.62, 596.13, 555.72, 514.42, and 473.94. For the 3:7ratio 3360.30 cm^{-1} OH stretching vibrations. Activated carbon improves the composite's ability to adsorb substances, which makes dye removal more effective. 1794.86 cm^{-1} reveals the carbonate species (CO_3^{2-}) that have been absorbed on the composite surface. Because carbonate ions encourage the

production of reactive oxygen species (ROS) during the breakdown of MB dye molecules, they can increase photocatalytic activity. The other peaks to symbolize different functional groups and molecular vibrations. These could contain new chemical modes, C-H bending vibrations, and stretching vibrations of OH. For the 1:1ratio 3641.06, 3345.06, 2511.52, 2184.27, 2099.46, 1974.73, 1794.92, .63, 1047.48, 873.30, 710.03, 462.60, and 432.27. 3641.06 cm $^{-1}$and3345.06 cm^{-1} are OH stretching vibrations. 2511.52 cm^{-1}aromatic C=C stretching vibrations. The other peaks represent various functional groups and molecular vibrations within the composite. The FTIR study of calcium oxide (CaO) and the composite CaO/AC (calcium carbonate, $CaCO_3$) is shown in Figure 4.6. The spectrum exhibits higher peaks.

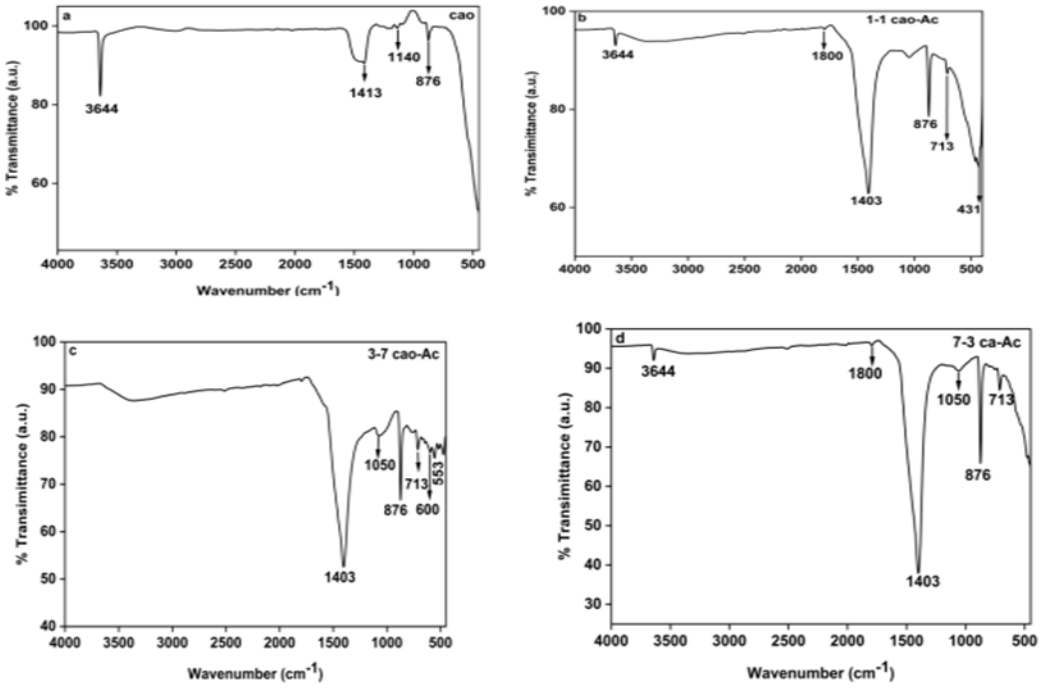

Figure 4. 6 FTIR analysis of CaO and composite of CaO with AC individual

The properties of the various calcined samples were defined by the distinct crystal structure, content, porosity, and particle shape of the $CaCO_3$. CaO was more likely to developed in the calcined sample due to the trigonal crystal system in $CaCO_3$, which also increased the carbonation conversion rate(Olivares-Marín *et al.*, 2013).

4.5 Photocatalytic studies.

The first study looked at how well CaO and a mixture of CaO and activated carbon could break down the light-absorbing Methylene Blue (MB) dye. First, an adsorption test was conducted in the dark with a mixture of catalyst and dye solution. After 30 minutes, samples were centrifuged and UV spectral data was analyzed where MB concentration remained the same. These were clear evidence that catalyst does not adsorb MB. After the adsorption studies, degradation experiment was carried out in reactor in order to find whether the catalyst could degrade the dye molecule. In UV spectra, the intensity of the absorption peaks decreases to minimum for MB due to the result of photocatalytic reaction. Under the light irradiation, MB turned to colorless solution within 15 min, it concludes that CaO have higher photodegradation efficiency on MB (Meshkatalsadat *et al*., 2022). Percentage of degradation calculated by Equation (1) and kinetic rate constant equation (2) that shown under section 3.5 above.

4.5.1. Effect of Catalyst mass (dosage).

The catalyst dose is an important parameter in photocatalytic degradation of organic dyes. Increase in the photo-catalyst dosage was increase the dye removal efficiency, as a result of multiplication of the active sites thereby increasing the active species concentration in the reaction mixture.

The efficiency ranges from 98.6 to 98.5 as the CaO catalyst concentration increases from 10 mg to 30mg. decrease by 0.01' CaO the highest kinetic rate constant ($5.42667*10^{-4}min^{-1}$) and correlation Coefficient (0.7157) at 10 mg catalyst were obtained as presented in Table 4.1. One of the potential causes for decreasing the catalytic activity at 30 mg could be the turbidity of the solution as a result of the increase in the amount of catalyst, which prevents radiation from entering the solution. Another factor could be the agglomeration of high concentrations of nanoparticles in the solution, which limits the number of active surface sites that are open to exposure(Jiang *et al.*, 2009).

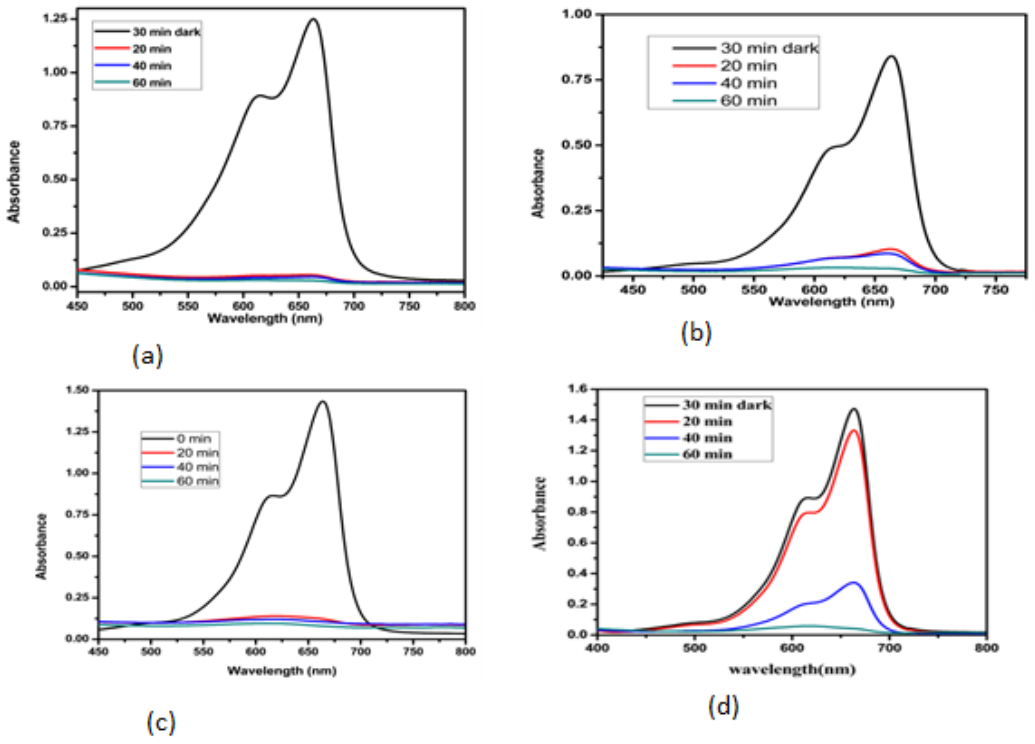

Figure 4. 7 Absorbance versus wavelength plots of catalyst CaO and composite of CaO with AC ($CaCO_3$) a) 10 mg of CaO b) 30 mg CaO, c) 10 mg of $CaCO_3$, d) 30 mg Oof $CaCO_3$

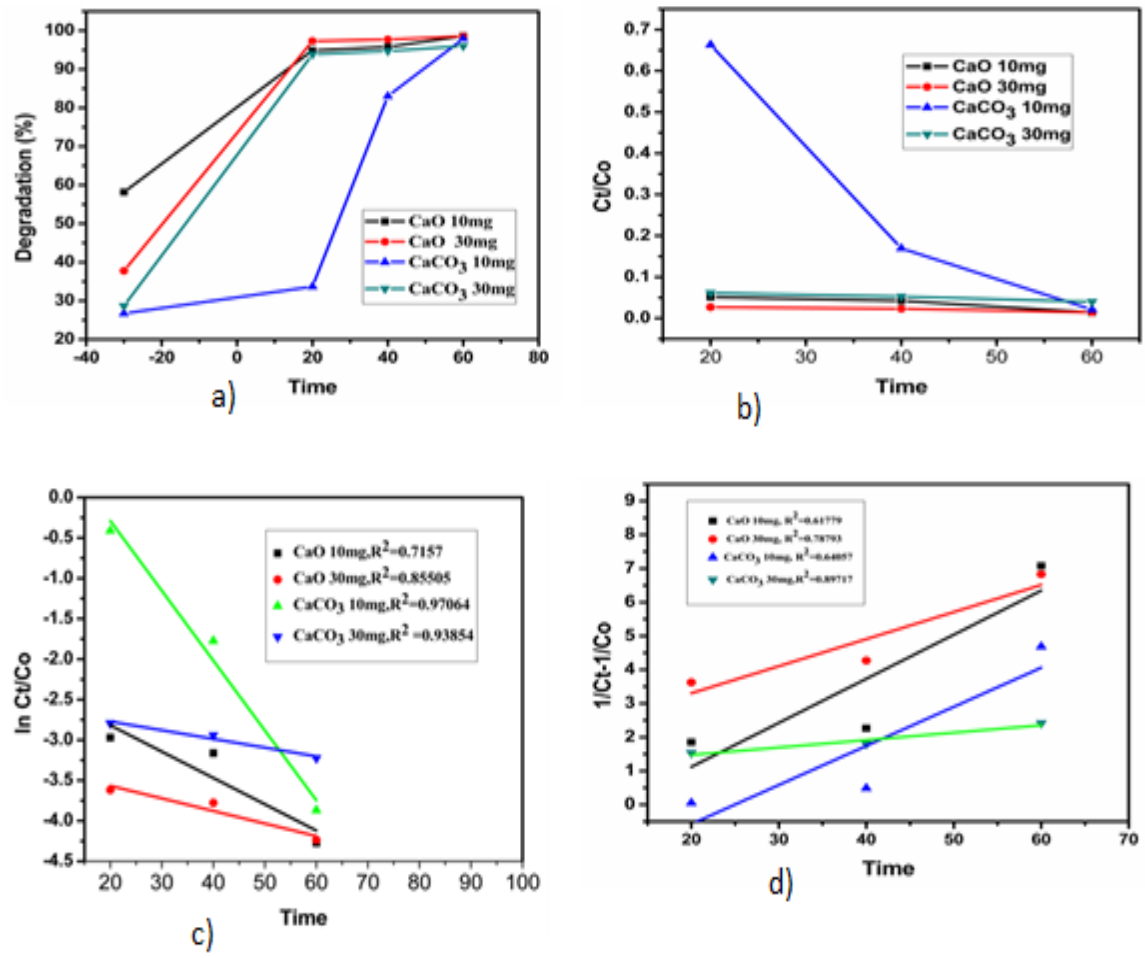

Figure 4. 8 a) is the percent degradation versus time plot of catalyst dosage b) Ct/Co versus time plot of dosage, and c) ln Ct/Co versus time pseudo-first order kinetics linear plots catalyst dosage, and d) pseudo-second-order kinetics.

4.5.2. Effect of pH

The pH of the solution is a critical factor for pollutant degradation. Solution of pH at 5 and 12 for the CaO and $CaCO_3$ catalyst was studied using HCl and NaOH for pH adjustment, as shown in Fig. 4.10. Most of the cationic dyes showed better efficiency at basic pH due to strong electrostatic interactions with the negative catalyst surface. The photocatalytic efficiency decreased with decreasing pH because of the electrostatic repulsion between the dye and the catalyst. Higher pH levels lead to greater formation of hydroxyl radicals, which are more effective in decomposing pollutants under basic conditions, which explains the enhanced degradation efficiency at higher pH levels (Koe *et al.*, 2019).

Fig. 4.11 displays the percentage degradation efficiency, Ct/Co versus time, and ln Ct/Co pseudo-first and second -order kinetics linear plots. In acidic solution, both MB and catalysts have a positive charge, which results in repulsion towards one another. Thus, there was not complete degradation at pH 5. However, at higher values of PH 12, the degradation efficiency increased as a result of electrostatic attraction between the negatively charged catalyst and the positively charged MB (Table 1)

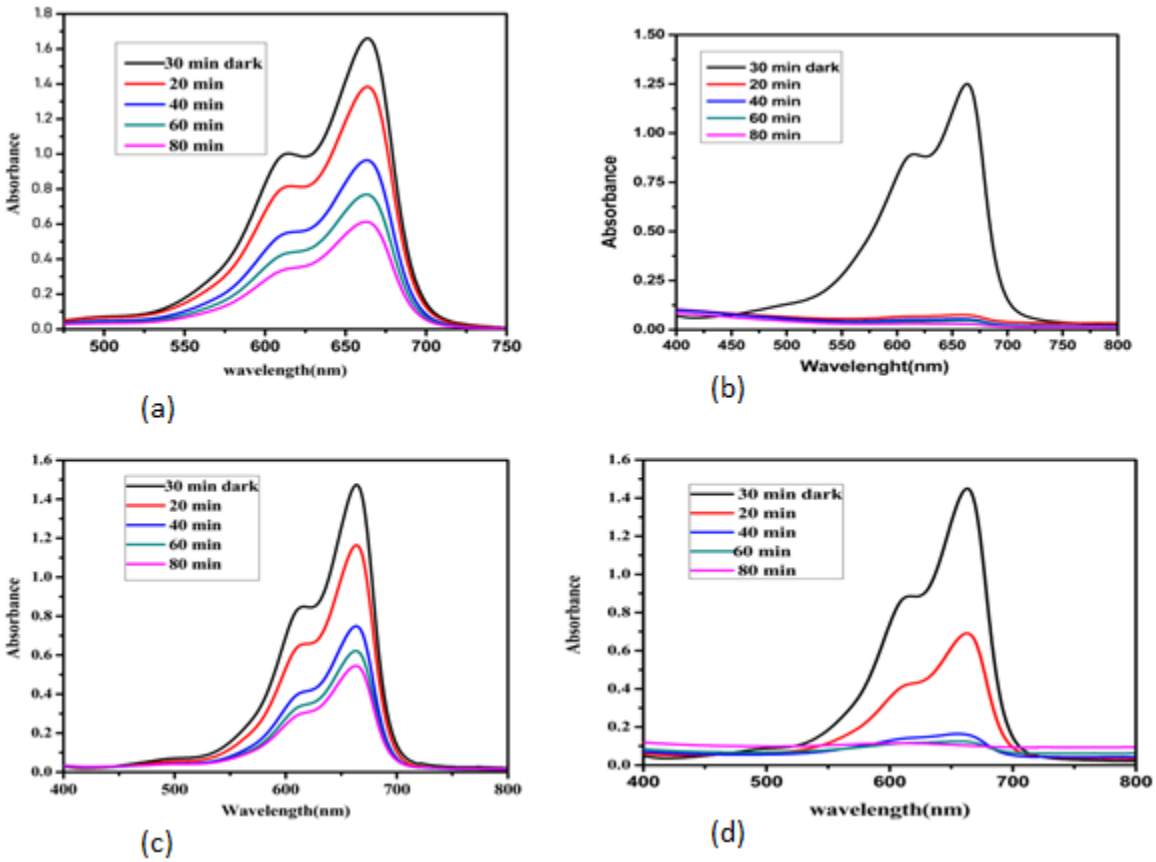

Figure 4. 9 Absorbance versus wavelength plots of catalyst CaO and composite of CaO and AC $CaCO_3$ a) pH 5.0 of CaO, b) pH 12 of CaO, c) pH 5.0 of $CaCO_3$, and d) pH 12.0 of $CaCO_3$

The comparison of photocatalytic efficiencies at PH 5 and pH 12 provides a thorough grasp of how pH affects the effectiveness of CaO and $CaCO_3$ in eliminating MB dye. In order to maximize photocatalytic degradation rates and efficiency, it aids in determining the ideal pH levels. The overall efficiency of the photocatalytic process is dependent on a number of factors, including ROS formation at varying pH levels, catalyst stability, and surface charge.

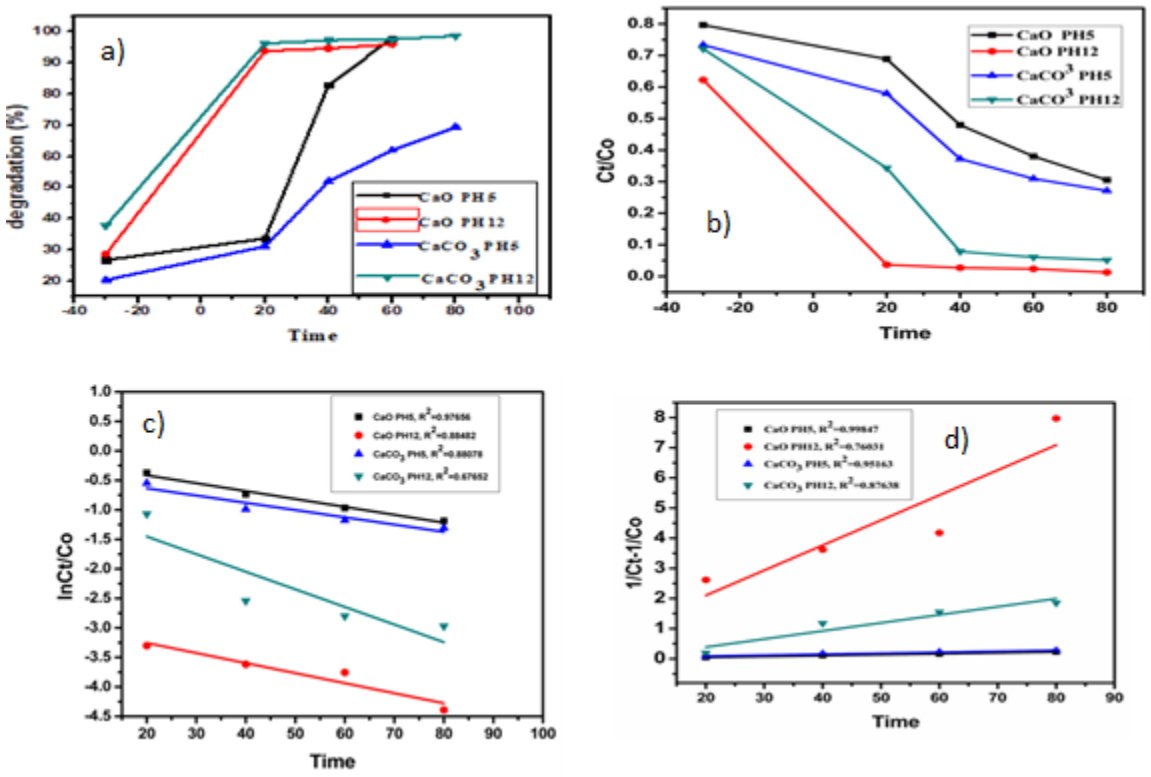

Figure: 4. 10. a) percent degradation versus time plot of pH 5, and 12 ;b) Ct/Co versus time plot of pH 5 and 12 and c) ln Ct/Co versus time pseudo-first-order kinetics linear plots of pH 5, and 12 d) second -order kinetics linear plots.

4.5.3. Effect of dye concentration

The amount of •OH radicals formation on the catalyst surface and interacted with the dye molecules represent the rate of degradation. Increase in dye concentration was reduce the reactive species concentration that will result in decrease in degradation efficiency and rate of reaction. Once, the amount of dye molecules increases, number of dye molecules for excitation and contact with the catalyst surface also increases. Thus, the quantity light penetrates into the solution, photon reach the surface of the catalyst was reduced and also more amount of light absorbed by the dye than the catalyst. Also, increase in dye concentration was result in the requirement of catalyst surface needed for better degradation. If reaction time and quantity of catalyst remain constant, then the •OH radical (primary oxidant) formed on the catalyst surface also remains constant. Thus the number of reactive groups cleaving the dye molecules decreases with increasing amount of the dye(Goswami *et al.*, 2023).

Fig. 4.12 shows the photocatalytic degradation of MB in the presence of CaO and composite of CaO and $CaCO_3$ catalyst with various initial dye concentrations (10 ppm, and 20 ppm) under light irradiation. The highest deterioration of CaO was achieved at 10 ppm, with the highest degradation efficacy of 98.5%. The obtained rate constant was $1.8925*10^{-4}$ min^{-1} with a correlation coefficient value of 0.94499, and for $CaCO_3$ as illustrated in Fig. 4.13a and Table 4.1. Due to the production of OH• radical on the catalyst's surface and the reaction between the dye molecule and OH• radical, the efficiency of degradation improved as the initial dye concentration increased.

However, additional increases in the initial dye concentration cause the catalyst's activity to diminish because the reaction between the dye molecule and the OH• radical is inhibited when more dye adsorbs to the surface of the catalyst, which lowers the generation of the OH• radical(Reza *et al*., 2017).

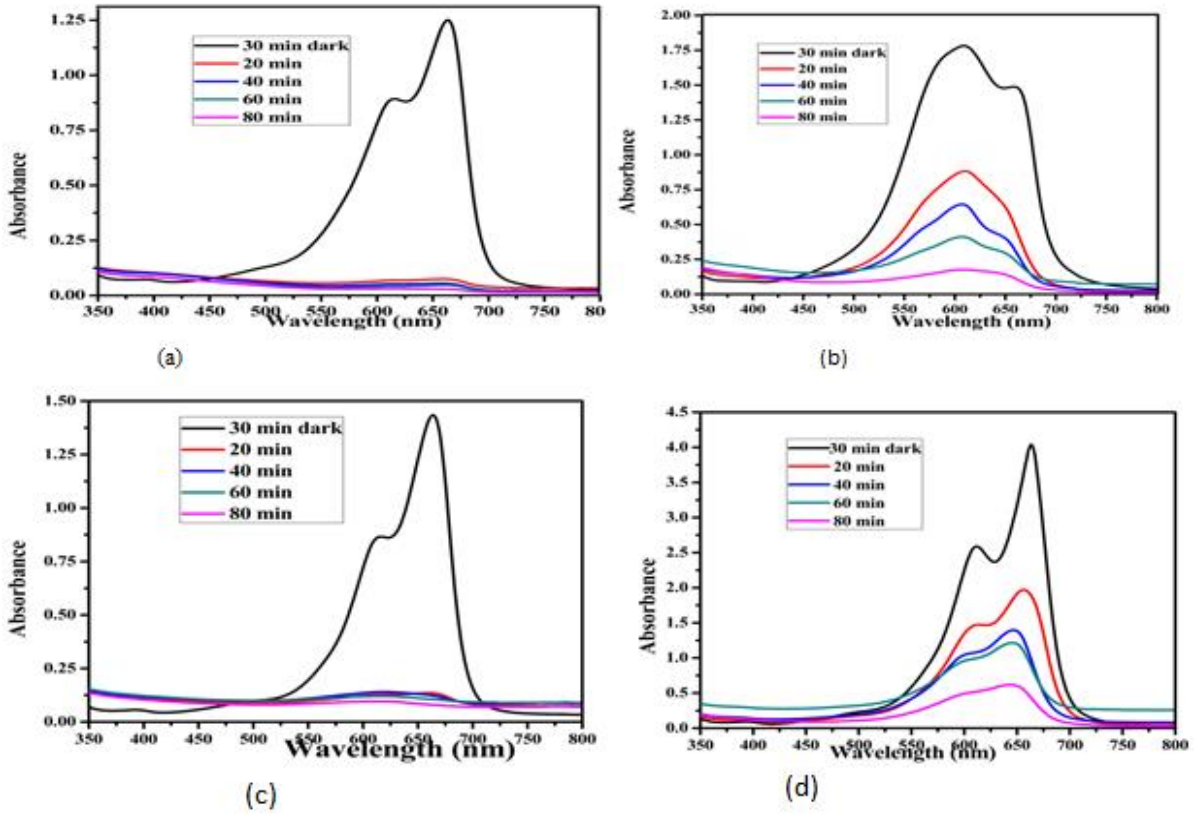

Figure 4. 11 Absorbance versus wavelength plots of methyl blue dye concentration a) CaO 10ppm, b) CaO 20ppm, c)$CaCO_3$ 10 ppm, d) $CaCO_3$ 20 ppm.

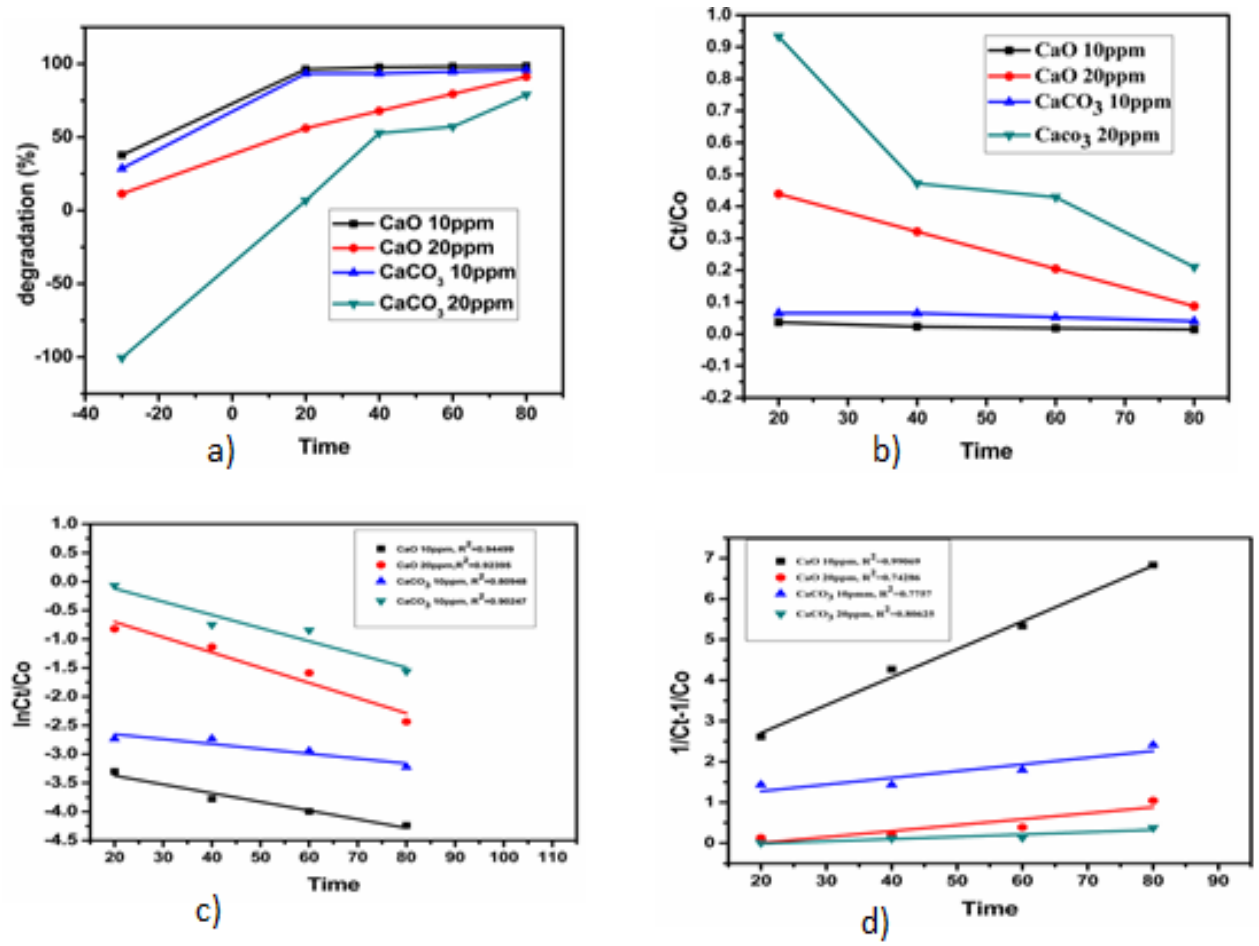

Figure 4. 12. a)) Percentage degradation b) Ct/Co versus time plot of 10 ppm, and 20 ppm; c) ln Ct/Co versus time pseudo-first-order kinetics linear plots of 10 ppm, and 20 ppm c) second order kinetics linear plots of 10ppm and 20pp

Table 4. 2 Percentage degradation efficiency, kinetic rate constant, and correlation coefficient of composites, catalyst dosage, pH of the solution, and initial concentration of the dye.

Catalyst Dosage				
	CaO		$CaCO_3$	
	10mg	30mg	10mg	30mg
PDE%	98.60	98.56	97.91	96.02
K(min^{-1})	$5.43*10^{-4}$	$2.59*10^{-4}$	$1.44*10^{-4}$	$1.79*10^{-4}$
R^2	0.7157	0.8550	0.9706	0.9385
PH of the solution				
	CaO		$CaCO_3$	
	5PH	12PH	5PH	12PH
PDE%	69.50	98.76	72.88	94.87
K(min^{-1})	$1.67*10^{-4}$	$2.13*10^{-4}$	$1.54*10^{-4}$	$3.73*10^{-4}$
R^2	0.9765	0.8848	0.8807	0.6765
Methyl blue concentration				
	CaO		$CaCO_3$	
	10ppm	20ppm	10ppm	20ppm
PDE%	98.55	91.24	96.02	79.00
K(min^{-1})	$8.9*10^{-4}$	$3.31*10^{-4}$	$1.06*10^{-4}$	$2.85*10^{-4}$
R^2	0.9450	0.9239	0.8095	0.9025

It is possible that the amount of active surface area available for photo catalytic reactions was decrease if $CaCO_3$ is formed on the surface of photo catalytic materials. This reduction may make active locations less accessible and reduce the overall effectiveness of the degradation of pollutants. When it comes to light absorption and scattering within the composite structure, $CaCO_3$ optical characteristics differ from those of photo-catalytic materials. The effectiveness of photo catalytic reactions, particularly in heterogeneous photo catalysis, may be impacted by this change in light distribution.

5. CONCLUSION AND RECOMMANDATION

5.1 Conclusion

In the present work CaO nanoparticle and activated carbon were successfully synthesized from eggshell and banana peel by solid state reaction respectively, and CaO-AC composite also prepared in the same manner. The CaO nanoparticles, Activated carbon and CaO-AC composite were characterized using analytical techniques such as TGA, XRD, FT-IR, SEM and UV-Visible spectrophotometry. XRD result confirmed the formation of cubic structure of CaO nanoparticles with crystallite size 59.5 nm. FT-IR spectra revealed characteristic peaks of Ca-O bonds and functional groups present in the synthase CaO NPs and CaO-AC composite ($CaCO_3$) responsible for the degradation of any organic functional group. From Photo catalytic degradation study, it is possible to conclude that the synthesized CaO nanoparticle and CaO-AC composite ($CaCO_3$) is efficient for degradation of methylene blue dye from wastewater under natural sun light irradiation. It was found that pH of the dye solution, catalyst dose, initial concentration of dye solution and exposure time has a great influence on the photo catalytic performance. The degradation efficiency of CaO NPs and CaO-AC composite ($CaCO_3$) against MB dye at pH 12, 10 gm of catalyst dose, and 50 mg/L of initial dye concentration was 98.76% within $2.13*10^{-4}$ minute Uv visible irradiation. The kinetic study indicates photo catalytic degradation of Methylene blue follows pseudo first order kinetics. Generally it is possible to conclude that CaO NPs and CaO-AC composite ($CaCO_3$) can be used for the degradation of methylene blue dye under Uv visible irradiation.

5.2 Recommendations

Synthesis of a CaO and activated carbon (AC) composite by utilizing an inert gas ensure the formation of pure CaO/AC composites. The use of inert gas such as nitrogen or argon, during the mixing and thermal decomposition process helps prevent unwanted reaction with atmospheric gases, such as oxygen, and carbon dioxide , which can lead to impurities in the final product. This optimization step is crucial for enhancing the photo catalytic efficiency of the CaO/AC composite by ensuring high purity and better interaction between the CaO and AC components. Present an assortment of experiments requiring a range of tools and methods. This strategy can let students use instruments more equally and lessen competition for certain resources. To reduce downtime and increase instrument availability, make sure that instruments are properly

maintained and repaired on time. Establish routine maintenance schedules and inspection schedules to avoid unplanned malfunctions.

ACKNOWLEDGEMENT

The research for this paper was financially supported by Adama Science and Technology University under the grant number of **ASTU/SM/R/1000/24**, Adama, Ethiopia.

REFERENCE

Abebe, B., Zereffa, E. A., & Murthy, H. C. A. (2021). Preparation of metal-polymer nanocomposites by chemical reduction of metal ions: functions of polymer matrices. *ACS Omega*, *6*(1), 954–964. https://doi.org/10.1021/acsomega.0c05597

Ali, M. H. H., Abdelkarim, M. S., & Al-Afify, A. D. G. (2024). Characterization and photodegradation of methylene blue dye using bio-synthesized cerium oxide nanoparticles with Spirulina platensis extract. *Discover Applied Sciences*, *6*(3). https://doi.org/10.1007/s42452-024-05736-1

Azbar, N., Yonar, T., & Kestioglu, K. (2004). Comparison of various advanced oxidation processes and chemical treatment methods for COD and color removal from a polyester and acetate fiber dyeing effluent. *Chemosphere*, *55*(1), 35–43. https://doi.org/10.1016/j.chemosphere.2003.10.046

Banković-Ilić, I. B., Miladinović, M. R., Stamenković, O. S., & Veljković, V. B. (2017). Application of nano CaO–based catalysts in biodiesel synthesis. *Renewable and Sustainable Energy Reviews*, *72*, 746–760. https://doi.org/10.1016/j.rser.2017.01.076

Bathla, A., Singla, D., & Pal, B. (2019). Highly efficient CaCO 3 -CaO extracted from tap water distillation for effective adsorption and photocatalytic degradation of malachite green dye. *Materials Research Bulletin*, *116*, 1–7. https://doi.org/10.1016/j.materresbull.2019.04.010

Bhagwat, V. R., Humbe, A. V., More, S. D., & Jadhav, K. M. (2019). Sol-gel auto combustion synthesis and characterizations of cobalt ferrite nanoparticles: Different fuels approach. *Materials Science and Engineering: B*, *248*(2), 114388. https://doi.org/10.1016/j.mseb.2019.114388

Bhatia, D., Sharma, N. R., Singh, J., & Kanwar, R. S. (2017). Biological methods for textile dye removal from wastewater: A review. *Critical Reviews in Environmental Science and Technology*, *47*(19), 1836–1876. https://doi.org/10.1080/10643389.2017.1393263

Boey, P. L., Maniam, G. P., & Hamid, S. A. (2011). Performance of calcium oxide as a heterogeneous catalyst in biodiesel production: A review. *Chemical Engineering Journal*, *168*(1), 15–22. https://doi.org/10.1016/j.cej.2011.01.009

Borhade, A. V., & Kale, A. S. (2017). Calcined eggshell as a cost effective material for removal of dyes from aqueous solution. *Applied Water Science*, *7*(8), 4255–4268. https://doi.org/10.1007/s13201-017-0558-9

Borhade, Ashok V., Tope, D. R., & Uphade, B. K. (2012). An efficient photocatalytic degradation of methyl blue dye by using synthesised PbO nanoparticles. *E-Journal of Chemistry*, *9*(2), 705–715. https://doi.org/10.1155/2012/362680

Chakhtouna, H., Benzeid, H., Zari, N., Qaiss, A. el kacem, & Bouhfid, R. (2021). Recent progress on Ag/TiO2 photocatalysts: photocatalytic and bactericidal behaviors. *Environmental Science and Pollution Research*, *28*(33), 44638–44666. https://doi.org/10.1007/s11356-021-14996-y

Chong, M. N., Jin, B., Chow, C. W. K., & Saint, C. (2010). Recent developments in photocatalytic water treatment technology: A review. *Water Research*, *44*(10), 2997–3027. https://doi.org/10.1016/j.watres.2010.02.039

Das, S., Kamat, P. V., Padmaja, S., Au, V., & Madison, S. A. (1999). Free radical induced oxidation of the azo dye Acid Yellow 9. *Journal of the Chemical Society. Perkin Transactions 2*, *6*, 1219–1223. https://doi.org/10.1039/a809720h

Dassanayake, R. S., Acharya, S., & Abidi, N. (2021). Recent advances in biopolymer-based dye removal technologies. *Molecules*, *26*(15). https://doi.org/10.3390/molecules26154697

Devarahosahalli Veeranna, K., Theeta Lakshamaiah, M., & Thimmasandra Narayan, R. (2014). Photocatalytic Degradation of Indigo Carmine Dye Using Calcium Oxide. *International Journal of Photochemistry*, *2014*, 1–6. https://doi.org/10.1155/2014/530570

FN, C., & MF, M. (2017). Factors Affecting Water Pollution: A Review. *Journal of Ecosystem & Ecography*, *07*(01), 5–8. https://doi.org/10.4172/2157-7625.1000225

Fraser, E. D. G., Dougill, A. J., Mabee, W. E., Reed, M., & McAlpine, P. (2006). Bottom up and top down: Analysis of participatory processes for sustainability indicator identification as a pathway to community empowerment and sustainable environmental management. *Journal of Environmental Management*, *78*(2), 114–127. https://doi.org/10.1016/j.jenvman.2005.04.009

Gikas, P., & Tchobanoglous, G. (2009). The role of satellite and decentralized strategies in water resources management. *Journal of Environmental Management*, *90*(1), 144–152. https://doi.org/10.1016/j.jenvman.2007.08.016

Gopalappa, H., Yogendra, K., Mahadevan, K. M., & Madhusudhana, N. (2012). A comparative Study on Photocatalytic Degradation of Violet GL2B azo Dye Using CaO and TiO2 Nanoparticles. *International Journal of Science Research*, *1*(2), 91–95.

https://doi.org/10.13140/RG.2.2.11328.17922

Goswami, Y. C., Kaundal, J. B., Begzaad, S., & Tiwari, R. K. (2023). Photocatalytic degradation of Methyl Red dye using highly efficient ZnO/CdS hierarchical heterostructures under white LED. *Journal of the Iranian Chemical Society*, *20*(7), 1681–1697. https://doi.org/10.1007/s13738-023-02789-8

Grzelczak, M., Vermant, J., Furst, E. M., & Liz-marza, L. M. (2010). *Directed Self-Assembly of Nanoparticles*. *4*(7), 3591–3605.

Gusain, R., Kumar, N., & Ray, S. S. (2020). Factors Influencing the Photocatalytic Activity of Photocatalysts in Wastewater Treatment. *Photocatalysts in Advanced Oxidation Processes for Wastewater Treatment*, 229–270. https://doi.org/10.1002/9781119631422.ch8

Habte, L., Shiferaw, N., Mulatu, D., & Thenepalli, T. (n.d.). *Synthesis of Nano-Calcium Oxide from Waste Eggshell by Sol-Gel Method*. 1–10.

Hadjiivanov, K. (2014). Identification and Characterization of Surface Hydroxyl Groups by Infrared Spectroscopy. In *Advances in Catalysis* (1st ed., Vol. 57). Elsevier Inc. https://doi.org/10.1016/B978-0-12-800127-1.00002-3

Hamad, H. N., & Idrus, S. (2022). Recent Developments in the Application of Bio-Waste-Derived Adsorbents for the Removal of Methylene Blue from Wastewater: A Review. *Polymers*, *14*(4). https://doi.org/10.3390/polym14040783

Hugo, W. B. (1995). A brief history of heat, chemical and radiation preservation and disinfection. *International Biodeterioration and Biodegradation*, *36*(3–4), 197–217. https://doi.org/10.1016/0964-8305(95)00055-0

Ismail, G. A., & Sakai, H. (2022). Review on effect of different type of dyes on advanced oxidation processes (AOPs) for textile color removal. *Chemosphere*, *291*. https://doi.org/10.1016/j.chemosphere.2021.132906

Jha, V. K., & Maharjan, J. (2022). Activated carbon obtained from banana peels for the removal of AS (III) from water. *Scientific World*, *15*(15), 145–157. https://doi.org/10.3126/sw.v15i15.45665

Jiang, J., Oberdörster, G., & Biswas, P. (2009). Characterization of size, surface charge, and agglomeration state of nanoparticle dispersions for toxicological studies. *Journal of Nanoparticle Research*, *11*(1), 77–89. https://doi.org/10.1007/s11051-008-9446-4

Kanade, K. G., Kale, B. B., Baeg, J. O., Lee, S. M., Lee, C. W., Moon, S. J., & Chang, H.

(2007). Self-assembled aligned Cu doped ZnO nanoparticles for photocatalytic hydrogen production under visible light irradiation. *Materials Chemistry and Physics*, *102*(1), 98–104. https://doi.org/10.1016/j.matchemphys.2006.11.012

Kasirajan, R., Bekele, A., & Girma, E. (2022). Adsorption of lead (Pb-II) using CaO-NPs synthesized by solgel process from hen eggshell: Response surface methodology for modeling, optimization and kinetic studies. *South African Journal of Chemical Engineering*, *40*(March), 209–229. https://doi.org/10.1016/j.sajce.2022.03.008

Kochito, J., Gure, A., Abdisa, N., Beyene, T. T., & Femi, O. E. (2024). Magnetic biochar nanocomposites of coffee husk and khat (Catha edulis) leftover for removal of Cr (VI) from wastewater. *Current Research in Green and Sustainable Chemistry*, *8*. https://doi.org/10.1016/j.crgsc.2024.100403

Koe, W. S., Lee, J. W., & Chong, W. C. (2019). An overview of photocatalytic degradation: photocatalysts, mechanisms, and development of photocatalytic membrane. *Colloid and Interface Science Journal*, 44.

Kumar, A. (2017). A Review on the Factors Affecting the Photocatalytic Degradation of Hazardous Materials. *Material Science & Engineering International Journal*, *1*(3), 106–114. https://doi.org/10.15406/mseij.2017.01.00018

Kuriakose, S., Satpati, B., & Mohapatra, S. (2015). Highly efficient photocatalytic degradation of organic dyes by Cu doped ZnO nanostructures. *Physical Chemistry Chemical Physics*, *17*(38), 25172–25181. https://doi.org/10.1039/c5cp01681a

Laysandra, L., Sari, M. W. M. K., Soetaredjo, F. E., Foe, K., Putro, J. N., Kurniawan, A., Ju, Y. H., & Ismadji, S. (2017). Adsorption and photocatalytic performance of bentonite-titanium dioxide composites for methylene blue and rhodamine B decoloration. *Heliyon*, *3*(12), e00488. https://doi.org/10.1016/j.heliyon.2017.e00488

Levine, J. (2020). Understanding Medical Cannabis. In *Understanding Medical Cannabis*. https://doi.org/10.4324/9780429343803

Lewoyehu, M. (2021). Comprehensive review on synthesis and application of activated carbon from agricultural residues for the remediation of venomous pollutants in wastewater. *Journal of Analytical and Applied Pyrolysis*, *159*(May), 105279. https://doi.org/10.1016/j.jaap.2021.105279

Lin, X., Burns, R. C., & Lawrance, G. A. (2005). Heavy metals in wastewater: The effect of

electrolyte composition on the precipitation of cadmium(II) using lime and magnesia. *Water, Air, and Soil Pollution*, *165*(1–4), 131–152. https://doi.org/10.1007/s11270-005-4640-9

Liu, Q. (2020). Pollution and Treatment of Dye Waste-Water. *IOP Conference Series: Earth and Environmental Science*, *514*(5). https://doi.org/10.1088/1755-1315/514/5/052001

Maia, L. of banana peel waste for producing activated carbon via N. and pyrolysis for methylene blue removala S., Duizit, L. D., Pinhatio, F. R., & Mulinari, D. R. (2021). Valuation of banana peel waste for producing activated carbon via NaOH and pyrolysis for methylene blue removal. *Carbon Letters*, *31*(4), 749–762. https://doi.org/10.1007/s42823-021-00226-5

Mashkoor, F., & Nasar, A. (2020). Magsorbents: Potential candidates in wastewater treatment technology – A review on the removal of methylene blue dye. *Journal of Magnetism and Magnetic Materials*, *500*, 166408. https://doi.org/10.1016/j.jmmm.2020.166408

Meshkatalsadat, M. H., Zahedifar, M., & Pouramiri, B. (2022). Facile green synthesis of CaO NPs using the Crataegus pontica C.Koch extract for photo-degradation of MB dye. *Environmental Science and Pollution Research*, *29*(36), 54688–54697. https://doi.org/10.1007/s11356-022-19671-4

Moradihamedani, P. (2022). Recent advances in dye removal from wastewater by membrane technology: a review. *Polymer Bulletin*, *79*(4), 2603–2631. https://doi.org/10.1007/s00289-021-03603-2

Mujtaba, G., Muhammad, N., Shah, Q., Khan, M., & Abbood, N. K. (2023). *Water Pollution Hazards and Toxicity Caused by Textile Industries Ef ? luent*. *7*(2), 22–27.

Nadew, T. T., Keana, M., Sisay, T., & Getye, B. (2023). Synthesis of activated carbon from banana peels for dye removal of an aqueous solution in textile industries: optimization, kinetics, and isotherm aspects. *Water Practice and Technology*, *18*(4), 947–966. https://doi.org/10.2166/wpt.2023.042

Nawaz, M. S., & Ahsan, M. (2014). Comparison of physico-chemical, advanced oxidation and biological techniques for the textile wastewater treatment. *Alexandria Engineering Journal*, *53*(3), 717–722. https://doi.org/10.1016/j.aej.2014.06.007

Olivares-Marín, M., Cuerda-Correa, E. M., Nieto-Sánchez, A., García, S., Pevida, C., & Román, S. (2013). Influence of morphology, porosity and crystal structure of CaCO3 precursors on the CO2 capture performance of CaO-derived sorbents. *Chemical Engineering Journal*,

217, 71–81. https://doi.org/10.1016/j.cej.2012.11.083

Remucal, C. K., & Manley, D. (2016). Emerging investigators series: The efficacy of chlorine photolysis as an advanced oxidation process for drinking water treatment. *Environmental Science: Water Research and Technology*, *2*(4), 565–579. https://doi.org/10.1039/c6ew00029k

Reza, K. M., Kurny, A., & Gulshan, F. (2017). Parameters affecting the photocatalytic degradation of dyes using TiO2: a review. *Applied Water Science*, *7*(4), 1569–1578. https://doi.org/10.1007/s13201-015-0367-y

Robinson, T., McMullan, G., Marchant, R., & Nigam, P. (2001). Remediation of dyes in textile effluent: A critical review on current treatment technologies with a proposed alternative. *Bioresource Technology*, *77*(3), 247–255. https://doi.org/10.1016/S0960-8524(00)00080-8

Saeed, M., Muneer, M., Haq, A. ul, & Akram, N. (2022). Photocatalysis: an effective tool for photodegradation of dyes—a review. *Environmental Science and Pollution Research*, *29*(1), 293–311. https://doi.org/10.1007/s11356-021-16389-7

Saggioro, E. M., Oliveira, A. S., Pavesi, T., Maia, C. G., Ferreira, L. F. V., & Moreira, J. C. (2011). Use of titanium dioxide photocatalysis on the remediation of model textile wastewaters containing azo dyes. *Molecules*, *16*(12), 10370–10386. https://doi.org/10.3390/molecules161210370

Saha, B., Chowdhury, S., Sanyal, D., Chattopadhyay, K., & Suresh Kumar, G. (2018). Comparative Study of Toluidine Blue O and Methylene Blue Binding to Lysozyme and Their Inhibitory Effects on Protein Aggregation. *ACS Omega*, *3*(3), 2588–2601. https://doi.org/10.1021/acsomega.7b01991

Sahadat Hossain, M., Jahan, S. A., & Ahmed, S. (2023). Crystallographic characterization of bio-waste material originated CaCO3, green-synthesized CaO and Ca(OH)2. *Results in Chemistry*, *5*(February). https://doi.org/10.1016/j.rechem.2023.100822

Sawant, S., Somani, S., Omanwar, S. K., & Somani, P. (2016). Chemical and Photocatalytic Degradation of Crystal Violet Dye by Indian Edible Chuna (Calcium Oxide/Hydroxide). *Journal of Green Science and Technology*, *2*(1), 45–48. https://doi.org/10.1166/jgst.2015.1038

Schirmer, R. H., Coulibaly, B., Stich, A., Scheiwein, M., Merkle, H., Eubel, J., Becker, K., Becher, H., Müller, O., Zich, T., Schiek, W., & Kouyaté, B. (2003). Methylene blue as an

antimalarial agent. *Redox Report*, *8*(5), 272–275. https://doi.org/10.1179/135100003225002899

Science, E. (2021). *The effect of CaO doping in activated carbon composite as a heavy metal adsorbent in water The effect of CaO doping in activated carbon composite as a heavy metal adsorbent in water*. https://doi.org/10.1088/1755-1315/718/1/012063

Soroush, S., Mahmoodi, N. M., Mohammadnezhad, B., & Karimi, A. (2022). Activated carbon (AC)-metal-organic framework (MOF) composite: Synthesis, characterization and dye removal. *Korean Journal of Chemical Engineering*, *39*(9), 2394–2404. https://doi.org/10.1007/s11814-022-1100-9

Taiwo Adewale M. (2011). Composting_as_A_Sustainable_Waste_Manage. In *Journal of Environmental Science and Technology*.

Tan, H., Li, J., He, M., Li, J., Zhi, D., Qin, F., & Zhang, C. (2021). Global evolution of research on green energy and environmental technologies:A bibliometric study. *Journal of Environmental Management*, *297*(July), 113382. https://doi.org/10.1016/j.jenvman.2021.113382

Todd, L. (2015). *Accepted manuscript Development Accepted manuscript*. *June*, 1–33.

Tomar, R., Abdala, A. A., Chaudhary, R. G., & Singh, N. B. (2020). Materials Today : Proceedings Photocatalytic degradation of dyes by nanomaterials. *Materials Today: Proceedings*, *xxxx*, 4–10. https://doi.org/10.1016/j.matpr.2020.04.144

Ukaogo, P. O., Ewuzie, U., & Onwuka, C. V. (2020). Environmental pollution: Causes, effects, and the remedies. In *Microorganisms for Sustainable Environment and Health*. INC. https://doi.org/10.1016/B978-0-12-819001-2.00021-8

Vanthana Sree, G., Nagaraaj, P., Kalanidhi, K., Aswathy, C. A., & Rajasekaran, P. (2020). Calcium oxide a sustainable photocatalyst derived from eggshell for efficient photo-degradation of organic pollutants. *Journal of Cleaner Production*, *270*, 122294. https://doi.org/10.1016/j.jclepro.2020.122294

Viena, V., Elvitriana, Nizar, M., Wardani, S., & Suhendrayatna. (2018). Preparation of activated carbons from banana (Musa acuminate l.) peels for carbon monoxide adsorption. *Emerald Reach Proceedings Series*, *1*, 381–386. https://doi.org/10.1108/978-1-78756-793-1-00087

Vishnu, D., Dhandapani, B., Authilingam, S., & Sivakumar, S. V. (2020). A Comprehensive Review of Effective Adsorbents Used for the Removal of Dyes from Wastewater. *Current*

Analytical Chemistry, *18*(3), 255–268. https://doi.org/10.2174/1573411016999200831111155

Xia, Y., Xiong, Y., Lim, B., & Skrabalak, S. E. (2009). Shape-controlled synthesis of metal nanocrystals: Simple chemistry meets complex physics? *Angewandte Chemie - International Edition*, *48*(1), 60–103. https://doi.org/10.1002/anie.200802248

Xie, A., Jin, M., Zhu, J., Zhou, Q., Fu, L., & Wu, W. (2023). Photocatalytic Technologies for Transformation and Degradation of Microplastics in the Environment: Current Achievements and Future Prospects. *Catalysts*, *13*(5). https://doi.org/10.3390/catal13050846

Yec, C. C., & Zeng, H. C. (2014). Synthesis of complex nanomaterials via Ostwald ripening. *Journal of Materials Chemistry A*, *2*(14), 4843–4851. https://doi.org/10.1039/c3ta14203e